



Cite this: *J. Mater. Chem. B*, 2022, 10, 7281

## Electrospun nanofibers for manipulating soft tissue regeneration

Xindan Zhang,<sup>†,ab</sup> Yuxuan Meng,<sup>†,ab</sup> Bowen Gong,<sup>ab</sup> Tong Wang,<sup>ab</sup> Yonglai Lu,<sup>ab</sup> Liqun Zhang<sup>id</sup><sup>ab</sup> and Jiajia Xue<sup>id</sup><sup>\*ab</sup>

Soft tissue damage is a common clinical problem that affects the lives of a large number of patients all over the world. It is of great importance to develop functional scaffolds to manipulate and promote the repair and regeneration of soft tissues. Owing to their unique composition and structural properties, electrospun nanofibers have attracted much attention for soft tissue regeneration. Electrospun nanofibers can be easily constructed and functionally modified to regulate their composition, morphology, structure, three-dimensional architecture, and biological functions, as well as specific light/electric/magnetic properties. By integrating multiple types of guidance cues, such as topographical and biochemical cues and external stimuli, electrospun nanofiber scaffolds can be used to manipulate cell behaviors and thus facilitate tissue regeneration. In this review article, we have first described the construction of electrospun nanofibers with specific morphology and topography and their capability of modulating cell migration, cell morphology, and stem cell differentiation. We have then discussed the role of electrospun nanofiber scaffolds in promoting the regeneration of different types of soft tissues, including nerves, skin, heart, blood vessels, and cornea, from the point of view of the anatomical structures and physiological regeneration processes of tissues. By presenting and discussing the recent progress of electrospun nanofibers in manipulating soft tissue regeneration, we hope to provide a possible solution and reference for the repair of tissue damage in clinical practice.

Received 21st March 2022,  
Accepted 7th May 2022

DOI: 10.1039/d2tb00609j

rsc.li/materials-b

### 1. Introduction

Due to the increasing incidence of tissue damage caused by mechanical injuries or cancers, the repair of damaged or injured tissues has become a major medical problem in the modern society. Most tissues are not self-healable, and scarring can be generated even after healing, which seriously hinders

<sup>a</sup> Beijing Laboratory of Biomedical Materials, Beijing University of Chemical Technology, Beijing 100029, P. R. China. E-mail: jiajiaxue@mail.buct.edu.cn

<sup>b</sup> State Key Laboratory of Organic-Inorganic Composites, Beijing University of Chemical Technology, Beijing 100029, P. R. China

<sup>†</sup> Xindan Zhang and Yuxuan Meng contributed equally to this work.



Xindan Zhang

Xindan Zhang was born in 1995 in Jilin City, Jilin Province. She received both her bachelor's degree and master's degree in Materials Science and Engineering from Beijing University of Chemical Technology. She is now pursuing her PhD degree at Beijing University of Chemical Technology with Prof. Jiajia Xue. Her research interest is focused on electrospun nanofibers for the repair of soft tissues, including skin, muscle, and spinal cord.



Yuxuan Meng

Yuxuan Meng was born in Inner Mongolia in 2000 and is currently pursuing her undergraduate degree at Beijing University of Chemical Technology with Prof. Jiajia Xue, majoring in polymer materials and engineering. Her research focuses on electrospun nanofibers for spinal cord injury repair.

the functional recovery of damaged tissues, affecting the quality of life of patients and causing a heavy socioeconomic burden.<sup>1–3</sup> In clinical practice, the most common treatments for tissue regeneration include autologous and allogeneic transplantation. Although there have been a large number of successful cases, autologous and allogeneic transplantation still suffers from insufficient donor area, secondary injury, susceptibility to infection, immune rejection, and limited donors.<sup>4</sup> Therefore, there is an urgent need to develop tissue regeneration strategies that are safer and more effective.

The development of tissue engineering and regenerative medicine has opened up a new era for tissue regeneration by applying the principles and methods from multiple disciplines such as life sciences, materials science, clinical medicine, computer science, and engineering to research and develop technologies for replacing, repairing, reconstructing or regenerating

human tissues.<sup>5</sup> Typically, it is a promising exploration to construct tissue regeneration scaffolds or artificial organs based on materials made of polymers, metals, ceramics, or their composites for *in vivo* implantation to promote the tissue regeneration.<sup>6</sup> To this end, the key to realize the scaffold-guided tissue regeneration is providing a tissue-mimicking environment for cell growth and development.<sup>7</sup> Cellular behavior is often regulated by the extracellular matrix (ECM) and biologically active factors.<sup>8</sup> ECM is an intricate network of macromolecules, which can provide suitable sites for cell survival and activity, manipulating cell morphology, metabolism, function, migration, proliferation and differentiation through signal transduction systems.<sup>9,10</sup> Therefore, constructing regenerative scaffolds that can mimic the structure and composition of the ECM is an important strategy to promote tissue regeneration.

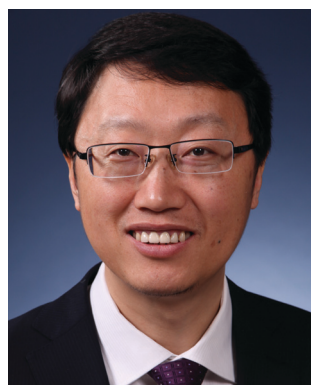
Owing to their capability of mimicking the structure and composition of the ECM, electrospun nanofibers have been widely applied as tissue regeneration scaffolds.<sup>11</sup> Many natural and synthetic polymers can be directly electrospun into nanofibers, conferring a diversity of electrospun fiber compositions.<sup>12</sup> Electrospun fibers range from tens of nanometers to a few micrometers in diameter, and they are stacked and connected to each other, with a large specific surface area and high porosity.<sup>13</sup> These properties allow electrospun fibers to provide a microenvironment that is conducive to cell development.<sup>14</sup> In addition, the physical parameters of electrospun fibers, such as composition, size, morphology, structure, strength, and function, can be well designed and regulated to meet the requirements of different tissues.<sup>15</sup> For example, electrospun fibers with different ordered structures can be obtained by varying the collection process to mimic the ordered structure of the ECM in various tissues. In addition, major components of the ECM such as laminin and fibronectin, as well as growth factors, genes, and drugs, can be deposited on the fiber surface or loaded into the fibers, imparting bioactivity and versatility to the scaffolds.<sup>16–18</sup> Thus, electrospun fibers can provide not only a fibrous structure and mechanical support,



**Yonglai Lu**

*Prof. Yonglai Lu obtained his BSc (1998) and MSc (2001) degrees from Beijing University of Chemical Technology and PhD (2004) from the Institute of Chemistry, Chinese Academy of Sciences. He has been a lecturer, an associate professor, and a professor in the College of Materials Science and Engineering at Beijing University of Chemical Technology since 2004. He worked as a visiting scholar at the State University of*

*New York at Stony Brook (2015.03–2015.09). His research interests include rubber nanocomposites, silicon elastomer materials for service under extreme conditions, thermally conductive elastomer composites, high-performance tires, etc.*



**Liqun Zhang**

*Prof. Liqun Zhang obtained his BSc (1990), MSc (1992), and PhD (1995) degrees from Beijing University of Chemical Technology. He has been a professor in the College of Materials Science and Engineering at Beijing University of Chemical Technology since 1995. He worked as a visiting scholar at the University of Akron (1990–2000) and then as a postdoctoral fellow at Case Western Reserve University (2000–2001). His research inter-*

*ests include rubber science and engineering, polymer nanocomposites, bio-based and biomedical materials, polymer processing engineering, etc.*



**Jiajia Xue**

*Prof. Jiajia Xue received her PhD in Materials Science and Engineering from Beijing University of Chemical Technology in 2015 with Prof. Liqun Zhang. She worked as a postdoctoral fellow in the Prof. Younan Xia's group at Georgia Institute of Technology from 2015 to 2019. She is now working as a professor at the Beijing University of Chemical Technology. Her research interests include the fabrication of nanomaterials and scaffolds for tissue engineering and regenerative medicine.*

but also chemical and biological cues to manipulate cell behavior and further promote tissue regeneration.<sup>19</sup>

In the human body, soft tissues, such as nervous system, heart, blood vessels, and so on, play important roles in supporting the functions of the body, and the injuries to soft tissues have a high incidence and are extremely common in clinics. The key elements for soft tissue regeneration are to reduce the inflammatory response, promote angiogenesis, and avoid scarring.<sup>20</sup> Electrospun nanofiber scaffolds have great potential in the field of soft tissue regeneration. In this review, we discuss the most recent progress on the construction of electrospun fibers for promoting and manipulating the regeneration of soft tissues, which mainly include nerve, skin, heart, blood vessels, and cornea. Cell behaviors have an important impact on the process of tissue regeneration, which are critical in determining the effectiveness of regeneration. We first describe the manipulation of cell behaviors by electrospun fibers. Then, we discuss the important role of electrospun fibers in different physiological processes of soft tissue repair. Finally, we present an outlook on the treatment of tissue injuries using electrospun fibers from the view of clinical needs.

## 2. Electrospun nanofibers for manipulating cell behaviors

The communication between cells and electrospun nanofibers is a dynamic and complex process. By varying the raw materials, parameters, and collection process of electrospinning, it is possible to obtain fibers with different properties according to the requirements, giving them functional versatility. Various biological and physicochemical properties of electrospun fibers are capable of inducing specific cellular responses. First, electrospun fibers can regulate the expression of integrins responsible for cell adhesion,<sup>21</sup> which is essential for regulating cell behaviors. Since electrospun fibers can mimic the structure and composition of the ECM to a certain extent, the adhesion of electrospun fibers to cells will contribute to cell migration, cell morphology, and stem cell differentiation. Adhesion is generally followed by cell migration, where both the speed and distance of cell migration are influenced by the structure and composition of the fibers. Electrospun fibers can also modulate cell morphology, which in turn alters intercellular communication and ultimately the function of the tissue. The properties of electrospun fibers can also affect cell differentiation.

### 2.1 Preparation and regulation of electrospun nanofibers

Electrospinning technology is widely used for the regeneration of different tissues due to its versatile process and the variable operability of polymers. A typical electrospinning device consists of a high voltage power supply, an injection pump, a spinneret, and a collector. During the electrospinning process, the liquid for electrospinning is extruded from the spinneret by the syringe pump to produce a dangling droplet. Upon energization with the application of a high voltage, the same charges will be accumulated on the surface of the droplet, and the electrostatic repulsion among the charges can deform the droplet

into a Taylor cone. By increasing the voltage to a critical value, an electrically charged jet will be ejected from the cone. The jet initially extends in a straight line and then undergoes a violent whipping motion due to bending instability. When deposited onto a grounded collector, the jets rapidly solidify into nanofibers.<sup>11,13,22</sup> When a flat device such as a piece of aluminium foil is used as the collector, the nanofibers will be deposited in a random fashion to form a non-woven membrane. By varying the shapes or architectures of the collectors, nanofibers will be deposited as different ordered structures. As shown in Fig. 1A, uniaxially aligned arrays of nanofibers can be collected by adjusting the mechanical forces using a highly rotated roller, electrostatic forces generated by using a U-shaped metal, or magnetic forces generated by a pair of permanent magnets, respectively. Radially aligned nanofibers can be prepared using a metal ring in the center and an array of metal pins or beads in the peripheral position.<sup>23</sup> A novel electrospinning technique was developed to prepare small diameter nanofiber conduits with different orientations at the same time. Two metal plates were placed a few centimeters apart, both connected to a DC negative voltage power supply. An electrically insulated Teflon rod connected to a rotating motor was introduced between the metal plates as a collector for the electrospun nanofibers. By changing the rotational speed, nanofibers of circumferential orientation and axial orientation could be collected simultaneously.<sup>24</sup> In addition, by controlling the electrospinning parameters, the fibers can be constructed to form a three-dimensional (3D) structure.<sup>25</sup> As shown in Fig. 1B, Eom *et al.* fabricated nanofibrous scaffolds with 3D structures by utilizing 3D-structured hydrogels as collectors instead of conventional metal collectors.<sup>26</sup>

The diameters of electrospun fibers are mainly in the range of 20–1000 nm, which can be effectively manipulated by adjusting the parameters of the electrospinning process including the applied voltage, the flow rate of the spinning fluid, and the distance between the spinneret tip and the collector, as well as environmental conditions such as temperature and humidity.<sup>27</sup> For example, a higher voltage is usually beneficial in reducing the fiber diameter. However, if the voltage is too high, it may also lead to an increase in fiber diameter by ejecting more liquid.<sup>28</sup> When the applied voltage is low, the generated electric field force is not high enough to overcome the surface tension of the spinning fluid, which prevents the stretching of the spinning fluid, thus increasing the fiber diameter. In addition, the flow rate of the spinning fluid also has an important effect on the fiber diameter. With the increase in the flow rate, the fiber diameter will be increased accordingly. The distance between the spinneret tip and the collector affects the electric field strength and the volatilization of the spinning fluid. When the distance is short, the insufficient evaporation of the solvent will result in a larger fiber diameter. With a longer spacing, the spinning fluid is sufficiently stretched, resulting in fibers with a smaller diameter.

The matrix type of electrospun nanofibers used for tissue regeneration greatly depends on the purpose of the study and the type of target cells and tissues. Natural polymers such as polysaccharides, gelatin, and collagen show suitable cell attachment

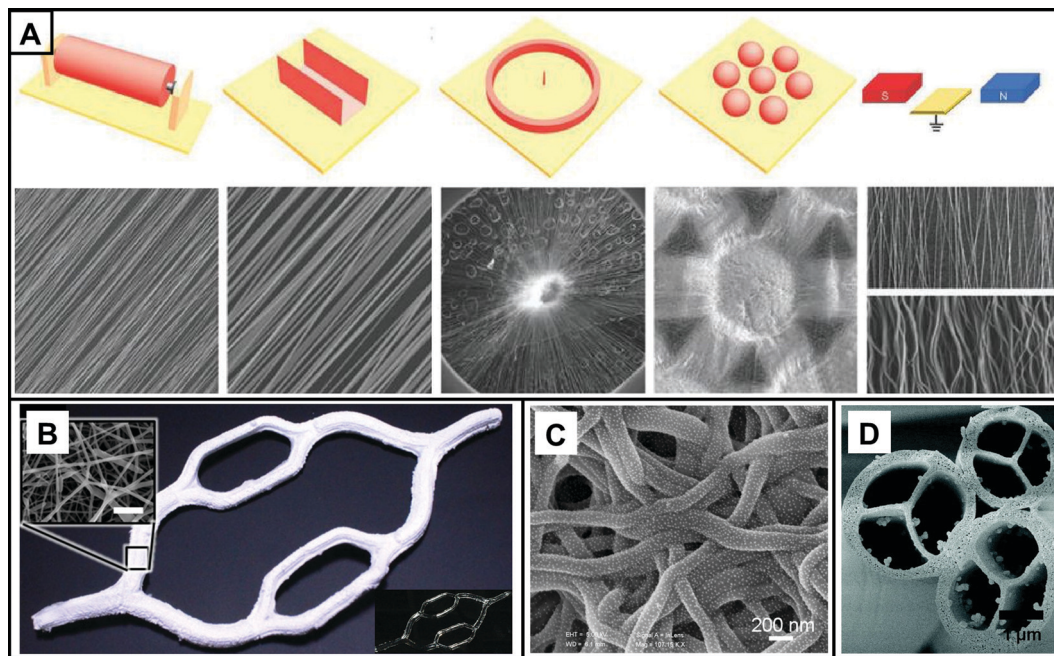


**Fig. 1** (A) Different collectors and SEM images of fibrous scaffolds prepared using the collectors. (B) 3D PCL nanofibrous scaffolds prepared using a 3D gelatin collector (bottom right) and SEM images of the surface (top left, scale bar = 5  $\mu\text{m}$ ). (C) SEM image of PVA fibers loaded with AuNPs. (D) SEM image of fibers with multiple channels. (A–D) Reprinted with permission from ref. 23: Copyright (2018) Elsevier, ref. 26: Copyright (2020) American Chemical Society, ref. 31: Copyright (2012) American Chemical Society, and ref. 32: Copyright (2007) American Chemical Society, respectively.

and differentiation, but their mechanical properties are often poor. Natural and synthetic materials can be mixed to produce composite fibers to combine the advantages of both types of materials. Different materials can also be combined to regulate the properties of the resultant fibers. For example, the modulus of poly( $\epsilon$ -caprolactone) (PCL) fibers can be decreased or increased by combining gelatin or polydimethylsiloxane with PCL, respectively.<sup>29</sup>

Porous fibers can be obtained by the phase separation between the soluble and insoluble components.<sup>30</sup> Small molecules or functional nanoparticles that are responsive to pH, enzyme, specific molecules, temperature, light, electrical or magnetic field can also be integrated to endow multiple functions to the fibers and the generated scaffolds. For example, gold nanoparticles (AuNPs) can be deposited on the surface of polyvinyl alcohol (PVA) fibers to allow them to be used as biosensor matrix materials (Fig. 1C).<sup>31</sup> It is also possible to form fibers with a core-sheath structure from two or more components through coaxial electrospinning. Such core-sheath fibers have a wide range of applications as controlled delivery systems. In addition, single- or multi-pore channel fibers can be formed when calcination of the core components occurs (Fig. 1D).<sup>32</sup> Electrospun fibers are simple to prepare and can be constructed into a variety of structures, from two-dimensional (2D) membranes to 3D tubes or porous scaffolds, playing an important role in modulating cell behavior and promoting tissue regeneration.

## 2.2 Cell migration

Cell migration is a complex process that involves several sequential steps of adhesion, polarization, and forward migration.<sup>33</sup> There are two main forms of cell migration: single migration

and collective migration.<sup>34</sup> In single cell migration, cytoskeleton reconstruction and posterior myosin contraction are the main causes of cell migration.<sup>35,36</sup> In collective cell migration, the leader cells are activated by soluble factors and interact with the ECM to produce polarization, and thus initiate cell migration. Collective cell migration is further driven by the interaction between the leader and follower cells (Fig. 2A).<sup>29</sup> Cell migration is an important cell behavior that plays a crucial role in the developmental and regeneration processes of tissues in the human body. Therefore, exploring the factors that can influence and manipulate cell migration has important implications in the design of electrospun nanofiber scaffolds for tissue regeneration.

Both topographical and biochemical cues of electrospun nanofibers are capable of providing signals for cell migration. An ordered arrangement of nanofibers can provide topographic cues for cell migration, manipulating their migration in specific directions and accelerating the rate of migration.<sup>37,38</sup> Random nanofibers are unable to provide directional guidance for cell migration, resulting in smaller displacements of cells in many different directions. In contrast, aligned nanofibers can provide specific directions and paths for cell migration through contact guidance, thereby increasing the rate of migration. Uniaxially aligned fibers can promote axial cell migration. For example, NIH-3T3 fibroblasts were cultured on normal tissue culture plates and uniaxially aligned PCL nanofibers, respectively.<sup>39</sup> After 9 days, the cells were stained to observe cell migration. As shown in Fig. 2B, the farthest migration distance of the cells on the uniaxially aligned nanofibers was significantly further than that on tissue culture plates. Moreover, the morphology of the cells at the forefront all showed a significant stretch along

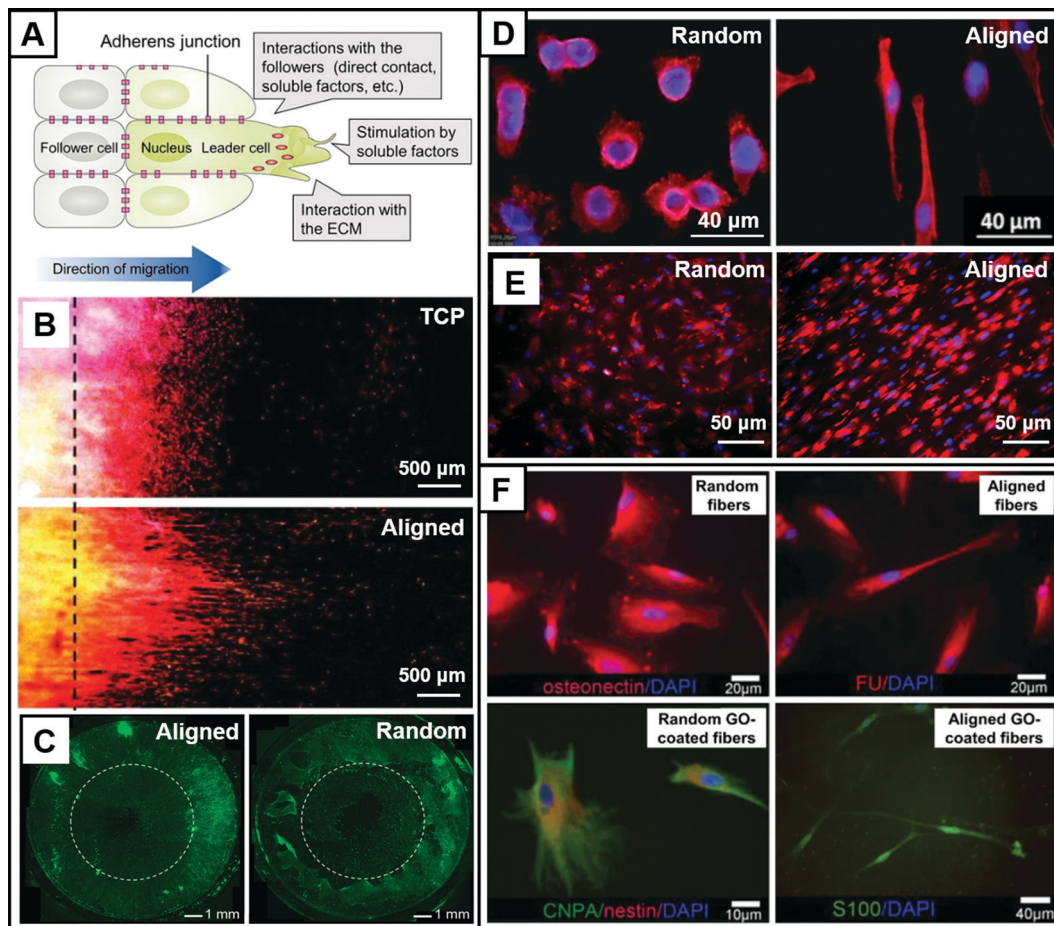


**Fig. 2** Modulation of cell behavior by electrospun nanofibers. (A) Mechanisms of collective cell migration. (B) Fluorescent fiber photographs showing linear migration of NIH-3T3 fibroblasts on control TCP and aligned scaffolds where the cell migration distance was significantly greater than that of the TCP group, demonstrating the facilitative effect of uniaxially arranged fibers on cell migration. DAPI (blue) stains the nucleus, anti-newtons (green) stains newtons, and ghost pen cyclin (red) stains F-actin. (C) Fibroblasts cultured on radially aligned nanofibers and randomly aligned nanofibers for 4 days; fibroblasts migrated from the periphery to the center along the radial direction of the nanofibers, reaching the center of the scaffold on the fourth day at a greater rate of migration than cells on randomly aligned nanofibers. Fibroblasts were stained with fluorescein diacetate. (D) Imaging revealed rounded keratin-forming cells on randomly oriented nanofibers, while keratin-forming cells on aligned uniaxial nanofibers showed elongated morphology and were oriented along the nanofibers. Nuclei were stained with Hoechst 33342 (blue) and actin filaments were stained with rhodamine ghost cyclopeptide (red). (E) SCs on random nanofibers were disorganized and did not form a regular cytoskeleton, and SCs on aligned nanofibers were uniformly oriented, showing a well-arranged actin network. The nuclei of SCs were stained with DAPI (blue), and the actin cytoskeleton was stained with rhodamine ghost pen cyclic peptide (red). (F) Neurospheres were cultured on randomly oriented electrospun nanofibers, aligned electrospun nanofibers, randomly electrospun fibers functionalized with GO, and aligned electrospun fibers functionalized with GO. It was demonstrated that the four different fiber morphologies and surface states resulted in the differentiation of DPSC neurospheres towards osteoblasts, glial cells, fibroblasts, and neurons, respectively. Neurospheres were immunofluorescently stained with osteoadhesive protein (red), nestin (red), CNPase (green), human fibroblast surface protein (FU) (red) and S100 (green), and DAPI (blue). (A–F) Reprinted with permission from ref. 29: Copyright (2018) American Institute of Physics, ref. 39: Copyright (2020) John Wiley and Sons, ref. 40: Copyright (2010) American Chemical Society, ref. 21: Copyright (2011) Elsevier, ref. 45: Copyright (2014) American Chemical Society, and ref. 51: Copyright (2018) John Wiley and Sons, respectively.

the axial direction. In addition, radially aligned nanofibers can promote radial cell migration. For instance, radially aligned PCL nanofibers were used to simulate the structure of the dura mater, and dural fibroblasts were cultured on random and radially aligned nanofibers, respectively.<sup>40</sup> On the radially aligned nanofibers, cells smoothly migrated radially from the periphery to the center of the nanofibers, while cells on the random fibers were unable to migrate to the center (Fig. 2C). This indicated that radial orientation could significantly accelerate and promote cell migration.

The surface chemistry of the aligned fibers and the growth factors released from the fibers can provide biochemical cues for cell migration. The combination of topographical cues and biochemical cues acts synergistically to further promote cell migration. For example, protein coating on the surface of aligned fibers can impart bioactivity to fibers, promote cell adhesion, and enhance cell–fiber interactions. Xie *et al.* cultured dural fibroblasts on random and radially aligned nanofibers with or without fibronectin coating.<sup>40</sup> The cell migration rate was highest when both orientation guidance and fibrin

coating existed simultaneously, demonstrating the role of protein coating on the surface on cell migration. Furthermore, if the bioactive substance on the aligned fiber surface has a gradient structure consistent with the orientation direction, it can confer stronger tropism to the cells, thus greatly facilitating cell migration. For example, biomacromolecular nanoparticles could be deposited on the surface of uniaxially aligned nanofibers by masked electrospraying to generate a unidirectional or bidirectional gradient of particle density.<sup>38</sup> Bone marrow stem cells (BMSCs) and NIH-3T3 fibroblasts were able to migrate in the direction of increasing particle density on the obtained nanofibers. The nanoparticles made of a mixture of collagen and fibronectin on the uniaxially aligned nanofibers in a bidirectional gradient density could promote the migration of Schwann cells (SCs) from the two sides to the center along the direction of increasing particle density. In another study, collagen nanoparticles were deposited in a radial density gradient on the surface of radially aligned nanofibers.<sup>41</sup> Migration of NIH-3T3 fibroblasts from the periphery to the center was facilitated by the dual effect of radial orientation and graded deposited protein.

In addition to the uniform or gradient deposition of the major proteins in the ECM on the fiber surface, growth factors can also be loaded into the fibers to induce cell migration. The manipulation of cell migration can be achieved through the controlled release of growth factors. Xue *et al.* sandwiched phase change material (PCM) particles loaded with epidermal growth factor (EGF) and the photothermal transformer indocyanine green (ICG) between two layers of radially aligned nanofibers and random nanofibers.<sup>39</sup> A size-tunable photo-mask was combined with near-infrared (NIR) light to trigger the solid-liquid phase transition of the PCM and thus the release of the EGF. The multilayered photothermal scaffold achieved a spatiotemporally controlled release of EGF, providing the growth factor on demand for cell migration. Cell migration along the radial direction was facilitated by the synergistic effect of the EGF and radiation orientation. The fiber topology, surface modification, and release of growth factors can be integrated to provide topographical and biochemical cues for cellular activity, modulate cell behavior, and promote cell migration.

### 2.3 Cell morphology

Due to the intrinsic structure and surface tension of a cell, as well as the external mechanical pressure, a cell always maintains certain morphology. The morphology of a cell is closely related to its function. For example, nerve cells will stretch over a long distance to facilitate the transmission of information from external stimuli. Some tissues of the human body, such as nerves, muscles, *etc.* display a high degree of cell order to maintain their structure and function. This directed cell growth can be achieved by applying aligned electrospun nanofibers.<sup>13</sup> For example, given that skeletal muscle was composed of parallel myotubular bundles formed by myoblasts, highly oriented nanofibers with micropatterns were prepared to guide the morphogenesis of muscle tissue. Through aligned

topographic cues, the nanofibers were able to modulate cytoskeletal alignment and myotubular assembly. The regeneration of muscle tissue was facilitated bottom-up from the nanoscale to the tissue level by moving from the alignment of cells to the formation of muscle tissue.<sup>42</sup> As shown in Fig. 2D, keratinocytes cultured on random nanofibers exhibited a circular morphology, while on aligned nanofibers, keratinocytes were spindle-shaped and exhibited an elongated morphology along the axial direction, and the cytoskeleton showed a high degree of orientation.<sup>21</sup> Furthermore, it has been shown that cells cultured on aligned nanofibers have greater stiffness and stronger cytoskeleton.<sup>43</sup>

The ability of cells to maintain their natural morphology after undergoing a range of cell behaviors is critical for tissue regeneration. In one study, tendon fibroblasts extended and aligned along the axial direction of the aligned nanofibers, forming a highly ordered structure that resembled the morphology of collagen fibers in tendons and creating good conditions for tendon tissue regeneration.<sup>44</sup> As another example, for the repair of peripheral nerve injury (PNI) using a conduit, the axially aligned nanofibers as the wall of the conduit alone cannot provide sufficient mechanical strength and are prone to tearing during surgery.<sup>45</sup> Therefore, a bilayer scaffold with good mechanical strength need be constructed by building a layer of random nanofibers on the outer layer of the aligned nanofibers. To verify whether the outer layer of random nanofibers would influence cell morphology, Xie *et al.* compared the cell morphology of SCs cultured on random nanofibers and aligned nanofibers.<sup>45</sup> As shown in Fig. 2E, SCs grown on random nanofibers were disordered and did not form a homogeneous actin network structure, whereas SCs on uniaxially aligned nanofibers had highly aligned and orientated morphology, forming a neat actin network.

Electrospun nanofibers can also induce changes in cell morphology by regulating gene expression. The aligned nanofibers can transmit certain mechanical stimulation signals and extracellular signals to the nucleus to trigger specific responses between cells and tissues, thus promoting the expression of some relevant genes and further influencing changes in cell morphology and cell behaviors.<sup>21</sup> The mechanism in this regard is still obscure and needs to be confirmed by further studies. In general, cell morphology plays a significant role in the repair of various tissues. Guiding cell deformation and extension by altering the morphology of electrospun nanofibers is of crucial importance in the field of tissue regeneration.

### 2.4 Stem cell differentiation

Stem cells are a class of cells that have the ability to self-renew, proliferate, and differentiate under certain conditions.<sup>46</sup> Stem cells are capable of differentiating into highly differentiated cells that make up the tissues and organs of the body, and also differentiate into progenitor cells.<sup>47,48</sup> Therefore, the behavior of stem cells, especially the directed differentiation of stem cells into specific types of cells, is crucial for tissue regeneration. The topographical features of the ECM act as an inducer of stem cell behavior, allowing them to change their phenotype according to

the microenvironment. Since electrospun nanofibers have an ECM-like structure, they can guide stem cell differentiation by mimicking the ecological niche of stem cells. Both the arrangement and diameter of electrospun nanofibers can influence stem cell differentiation. In one study, adipose-derived mesenchymal stem cells (ADSCs) on uniaxially aligned nanofibers were prone to directionally osteogenic differentiation relative to random nanofibers.<sup>49</sup> In another study, researchers explored the regulation of nanofiber diameter on the directional differentiation of neural stem cells (NSCs).<sup>50</sup> When the nanofiber diameter was about 280 nm, NSCs tended to differentiate into oligodendrocytes. As the nanofiber diameter increased, NSCs preferentially differentiated into neuronal lineages.

Stem cell differentiation can also be guided by surface modification of electrospun nanofibers. For example, primary neurospheres of dental pulp stem cells (DPSCs) were cultured on electrospun nanofibers modified with graphene oxide (GO) to explore stem cell differentiation on nanofibers.<sup>51</sup> Different topographical cues and surface modifications were able to modulate stem cell differentiation in different directions. On pristine random and uniaxially aligned nanofibers, and GO-coated random and uniaxially aligned nanofibers, neurospheres of DPSCs could be directionally differentiated into osteoblasts, glial cells, fibroblasts, and neurons, respectively (Fig. 2F). In addition, electrospun nanofibers can also modulate stem cell differentiation by combining with biochemical cues to modulate differentiation pathways by activating the recruitment and phosphorylation of focal adhesion kinases.<sup>52</sup> For example, osteogenic differentiation of mesenchymal stem cells (MSCs) could be significantly promoted by incorporating bone morphogenetic protein 2 and hydroxyapatite into electrospun nanofibers.<sup>53–55</sup> Culturing MSCs on PCL electrospun nanofibers loaded with retinoic acid could modulate the differentiation of MSCs toward the neuronal lineage.<sup>56,57</sup> By encapsulating vascular endothelial growth factor (VEGF) in gelatin particles which are then loaded into electrospun PCL nanofibers, the obtained scaffolds could promote the directed differentiation of MSCs into tubular endothelial cells.<sup>58</sup>

Since many cells are quite sensitive to electrical signals, the differentiation of stem cells can also be regulated by combining electrochemical signals with nanofibers. For example, induced pluripotent stem cells (iPSCs) were cultured on uniaxially aligned electrospun nanofibers made of polyaniline (PANI) and polyether-sulfone. The nanofibers induced the differentiation of iPSCs into cardiomyocytes by externally applied pulses mimicking electrical stimulation in the heart.<sup>59</sup> In addition, the use of piezoelectric materials could facilitate osteogenic differentiation of interstitial MSCs by generating an electroactive microenvironment without an external power source.<sup>60</sup> Electrospun nanofibers can further induce the directed differentiation of stem cells by combining topographical cues and biochemical cues. In tissue regeneration, depending on the tissue and repair purpose, electrospun nanofiber scaffolds with specific functions can be designed to provide a specifically tailored strategy for the regeneration of the target tissue. Electrospun nanofibers have outstanding advantages in tissue regeneration due to their targeted regulation of stem cell differentiation.

### 3. Electrospun nanofibers for manipulating soft tissue regeneration

Through modulation of cellular behavior, electrospun fibers can further manipulate soft tissue regeneration. It is essential to design electrospun fiber scaffolds with an optimized structure and function based on the specific ECM properties of different tissues for soft tissue regeneration. For example, aligned fibers play a specific role in guiding cell migration, differentiation, and morphology. Such scaffolds are commonly used in the regeneration of tissues with an ordered anatomical structure, including nerve, skin, heart, and blood vessels. In addition, by functionalization with bioactive substances such as growth factors, trophic factors, and proteins, the scaffolds can be further endowed with biomimetic ECM properties to provide a favorable microenvironment for tissue regeneration. The electrospun fiber scaffolds can also serve as a carrier of exogenous cells, addressing the shortcomings of cell therapy *via* injection.

#### 3.1 Peripheral nerve regeneration

Peripheral nervous system controls the sensory and movement of the human body. The anatomical structure of a peripheral nerve shows a cable-like structure. Each axon in the nerve fiber is surrounded by the nerve endoneurium, and the nerve fiber bundle is in turn covered by the nerve bundle membrane. Finally, the nerve consisting of nerve fiber bundles is wrapped by the nerve epineurium. PNI is a global medical problem. When peripheral nerves are injured, Wallerian degeneration first occurs at the damaged site.<sup>61</sup> Dedifferentiated SCs recruit macrophages to clear damaged tissue fragments. Macrophages also release VEGF-A to promote vascularization.<sup>62</sup> The clearance of inflammation and regenerated microvessels provide a favorable microenvironment for peripheral nerve regeneration. Afterwards, SCs migrate and proliferate massively, forming Büngner bands to pave the way for the extension of axons from the proximal stump to the distal stump.<sup>63</sup> At the same time, SCs release a variety of neurotrophic factors, such as nerve growth factor (NGF), brain-derived neurotrophic factor (BDNF), and neurotrophin-3 (NT-3), to further accelerate the axon to cross the damaged site and bridge the distal stump.<sup>64</sup> After successful bridging of the proximal and distal stumps, the SCs will remyelinate and motor or sensory function will be partially restored.

Although peripheral nerves can regenerate, their ability to regenerate is limited. Therefore, external intervention is required to repair PNI. End-to-end sutures are used clinically to treat PNI with small gaps.<sup>65</sup> When the gaps are large, the sutures will create more tension, resulting in the failure of nerve repair. Autografts are often used to repair large gap defects, which are the “golden standard” for repairing PNI.<sup>66</sup> However, autografts have disadvantages such as insufficient donors, secondary injury, and mismatch between donor and recipient nerve sizes.<sup>67</sup> Therefore, nerve conduits (NGCs) have been developed as neural tissue engineering scaffolds for the treatment of PNI.<sup>11</sup> The modulation of neuronal cell behavior by scaffolds can be facilitated by

modulating the structure and surface morphology of electrospun fibers. The combination of electrospun fiber-based NGCs with physical and biochemical cues can confer a broader range of functions to the scaffolds. For example, the delivery of active substances can suppress local inflammation and establish a microenvironment that promotes nerve regeneration. Additionally, in combination with cell therapy, it can promote the growth of SCs and the extension of neurites. Besides, the introduction of external electrical stimulation is also more conducive to the remyelination of SCs, which is beneficial for promoting the recovery of nerve function.

**3.1.1 Construction of a regenerative environment.** Inhibition of inflammation and promotion of vascularization are the keys to provide a favorable microenvironment for peripheral nerve regeneration. The diameter, porosity, and arrangement of electrospun fiber scaffolds can effectively modulate the phenotype of macrophages. Scaffolds with large diameter and high porosity could induce macrophages differentiation into an anti-inflammatory (M2) phenotype, whereas macrophages cultured

on fibrous scaffolds with small diameter and low porosity exhibited a pro-inflammatory (M1) phenotype.<sup>68</sup> Random nanofibers induced the formation of M1 phenotype macrophages, whereas aligned nanofibers promoted the differentiation of macrophages to the repair-promoting M2 phenotype by guiding macrophages to extend directionally along the nanofibers.<sup>69</sup> As shown in Fig. 3A, Dong *et al.* fabricated an NGC by filling oriented microfibers inside a conduit composed of random nanofibers to repair a 10 mm sciatic nerve defect in rats.<sup>70</sup> The immunofluorescence images showed that more macrophages (CD68<sup>+</sup>) were recruited to the lesion site on day 7 in the group treated with nanofibrous conduits filled with ordered microfibers compared to those in the unfilled conduit group. More importantly, ordered microfibers also promoted the differentiation of macrophages towards the M2 phenotype (CD206<sup>+</sup>), while random nanofibers enabled macrophages to exhibit the M1 phenotype (iNOS<sup>+</sup>). Macrophages with M2 phenotype promoted SC migration, myelination, and axonal elongation, thereby enhancing the efficacy of PNI repair.

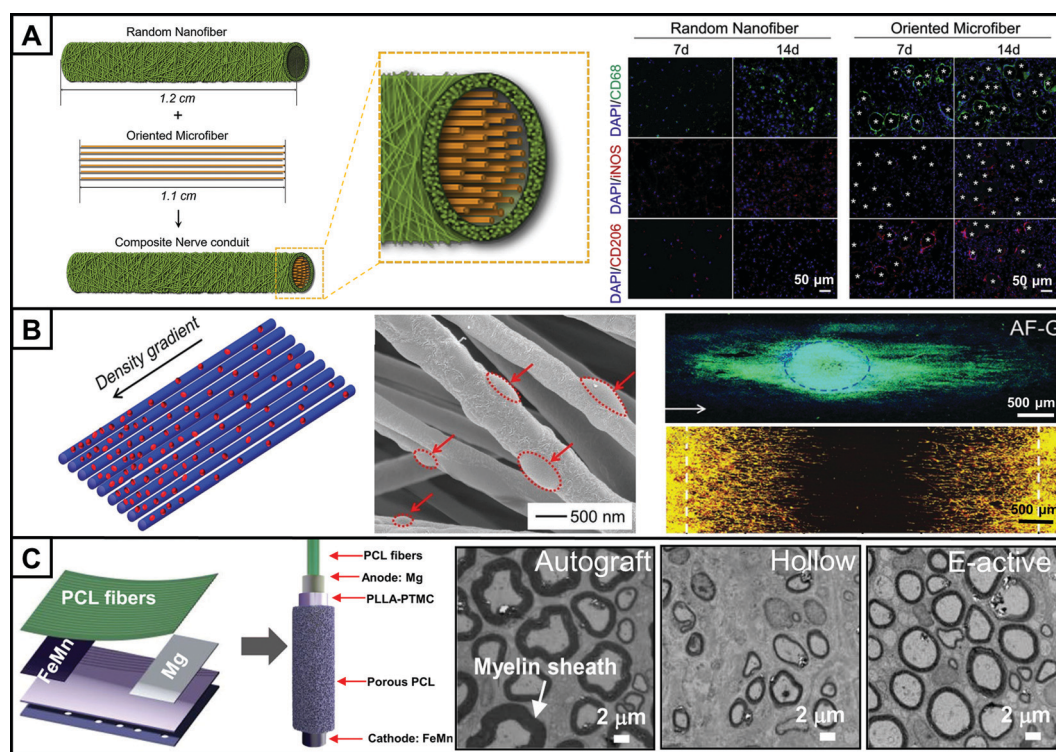


**Fig. 3** (A) Schematic illustration (left) of the effect of polarized macrophages on SC migration on different substrates. Macrophage polarization within the explanted conduits is characterized by immunofluorescent staining (right) for CD68 (M0, pan-macrophage, green), iNOS (M1, pro-inflammatory, red) and CD206 (M2, anti-inflammatory, red). The asterisks represent oriented microfibers. (B) Schematic illustration (left) and scanning electron microscopy (SEM) imaging (middle) showing the distribution of nanoparticles on uniaxially aligned nanofibers in a unidirectional density gradient. Fluorescence micrograph (top right) showing the neurites extending from DRG bodies on the graded scaffold. The white arrowed line indicates the direction of increasing the density of the nanoparticles. The neurites from DRG bodies were stained with Tuj1 (green), and the cell nuclei were stained with DAPI (blue). Fluorescence micrograph (bottom right) showing the migration of SCs from the two ends towards the center on the graded scaffold on which the density of nanoparticles increased from the two sides to the center. The actin cytoskeleton and the vinculin were stained with Alexa Fluor 555 phalloidin (red) and Alexa Fluor 488 anti-vinculin (green), respectively, and the yellow color corresponded to an overlay of these two colors. (C) Schematic illustration (left) of a biodegradable, self-electrified, and miniaturized conduit and transmission electron microscopy (TEM) images (right) of the middle sections of regenerated nerves when autograft, hollow conduit, and electroactive conduit group (E-active) were implanted to repair a 10 mm rat sciatic nerve injury, respectively. (A–C) Reprinted with permission from ref. 70: Copyright (2021) Elsevier, ref. 38: Copyright (2020) John Wiley and Sons, ref. 89: Copyright (2020) The American Association for the Advancement of Science, respectively.



In addition to adjusting their morphological parameters, electrospun fiber scaffolds can also be combined with anti-inflammatory or angiogenic substances to create a regenerative microenvironment. For example, interleukin 10 (IL-10), a cytokine that can promote the entry of macrophages into the M2 phenotype, could be covalently bound to PCL nanofiber scaffolds. When the scaffold was implanted around the damaged sciatic nerve, IL-10 was immobilized for up to 14 days, sufficient to downregulate the early inflammation reaction at the injury site.<sup>71</sup> Melatonin and Fe<sub>3</sub>O<sub>4</sub> magnetic nanoparticles encapsulated in the NGC wall could effectively inhibit oxidative stress and inflammation while guide axonal regeneration and remyelination. *In vivo* morphological and electrophysiological assessments demonstrated that the repaired nerves using the NGC were similar to those of the autograft group.<sup>72</sup> In addition, collagen IV filled in the tube could effectively modulate the phenotype of macrophages and inhibit inflammation, creating a suitable microenvironment for nerve regeneration.<sup>73</sup> Successful inhibition of inflammation is only the first step in promoting peripheral nerve regeneration. Direct regulation of axon extension and SC migration plays a crucial role in the process of nerve regeneration.

**3.1.2 Schwann cell growth and neurite extension.** The proliferation of SCs and extension of axons are the following crucial steps in peripheral nerve regeneration. After SCs migrate to the injury site and undergo massive proliferation, axons begin to extend under the wrapping of SCs. Aligned electrospun nanofibers have been widely used in neural tissue engineering to induce endogenous SC growth and axonal extension.<sup>74</sup> Electrospun fibers can be further modified to provide more topological cues such as pores, grooves or other secondary structures to modulate cell behaviors, thus improving the efficacy of PNI repair.<sup>75</sup> Wu *et al.* prepared PCL/poly(vinylpyrrolidone) (PVP) fibers with grooves on the surface by emulsion electrospinning.<sup>38</sup> The removal of PVP with ethanol successfully formed nanoscale grooves on each individual microfiber. Such microfibers with nanogrooves could provide more topographic contacts to growth cones, which further guided and promoted neurite outgrowth. The roughness of the scaffold surface also affects neurite extension. Electrospayed particles could be deposited on the surface of electrospun fiber scaffolds to adjust the surface roughness, and a suitable density of particles could promote neurite extension by providing appropriate anchor points for the growth cones.<sup>76</sup> In addition, multi-channel NGC could also provide more support and topological cues for cell growth and axon extension by mimicking the multiple fascicular structure of peripheral nerves compared to a single tubular conduit.<sup>77,78</sup> In one study, electrospun fiber membranes made of shape memory polymers were flattened at 25 °C, curled into tubes at 37 °C, and then self-assembled into a multi-channel conduit.<sup>78</sup> The multi-channel conduit promoted cell growth and axonal elongation during peripheral nerve regeneration and provided topographical cues for vascularity.

Combining electrospun fibers with bioactive effectors can further upgrade NGCs to provide biochemical cues to cells. These biological effectors include growth factors, trophic factors,

proteins and even the ECM.<sup>79,80</sup> For example, cross-linked laminin on aligned nanofibers enhanced axonal extension by providing both topological and biological cues.<sup>81</sup> Neural tissue decellularized matrix coated nanofibers could promote neuronal growth and SC migration by providing an ECM-like environment.<sup>82</sup> The concentration gradient of biological effectors, like collagen, fibronectin and NGF, also affects cell behaviors and axon extension owing to chemotaxis and haptotaxis effects.<sup>83</sup> In one study, nanoparticles made of a mixture of collagen and fibronectin were deposited in a density gradient on uniaxially aligned fibers by electrospaying.<sup>38</sup> The scaffolds promoted neuronal extension of the dorsal root ganglion (DRG) along the direction of increasing particle density (Fig. 3B). The bidirectional gradient of the particle density on the scaffold promoted the migration of SCs from the two sides with a low-density deposition toward the center with a high-density deposition. Controlled release of bioeffectors is important to improve their utilization efficiency and to achieve an on-demand supply at specific times after surgery. Xue *et al.* fabricated a scaffold with a three-layer structure by sandwiching NGF and a photothermal agent loaded in PCM particles between two layers of electrospun fibers. The controlled release of NGF was achieved by irradiation with a NIR light.<sup>18</sup> Combined with a photomask, the spatiotemporally controlled release of NGF could further enhance neurite extension.<sup>39</sup>

Topology and surface modifications of electrospun fibers, as well as loading of bioactive effectors, can promote the endogenous SC growth and neurite extension. In addition, exogenous SCs or stem cells can be introduced to the electrospun fiber scaffold to promote peripheral nerve regeneration by directly supplementing SCs or modulating the directional differentiation of stem cells to SCs. Wu *et al.* loaded SCs onto an electrospun chitosan scaffold.<sup>84</sup> In the *in vitro* experiments, the SCs formed a Büngner band-like structure on the scaffold and secreted BDNF that promoted nerve regeneration. This scaffold would greatly promote axonal extension after implantation *in vivo*. However, the SCs used for transplantation are often extracted from autologous peripheral nerves, which have poor proliferative capacity and are more injurious to the donor site. Therefore, providing other sources of SCs is an important alternative. A variety of stem cells can be differentiated into SCs, such as BMSC, ADSC, iPSC and so on. Peripheral nerve regeneration can be promoted by transplanting BMSCs into the body and modulating the directed differentiation of BMSCs to SCs. BMSCs could also be differentiated into SCs on electrospun fibers, and uniaxially aligned fibers could effectively regulate the differentiation of BMSCs into SCs and enhance the secretion of neurotrophic factors, which significantly promoted neurite extension.<sup>85</sup> Therefore, electrospun fibrous scaffolds loaded with exogenous cells have great potential in PNI repair.

**3.1.3 Functional recovery.** The goal of peripheral nerve regeneration is for functional recovery. Therefore, electrospun fiber scaffolds need to be further functionalized to facilitate re-establishment of bridges between nerves and other tissues *in vivo*. When the axon successfully bridges the proximal stump

and the distal stump, SCs will differentiate into myelin to wrap the axon, and peripheral nerve function will gradually recover. Appropriate myelin thickness and axonal diameter are the keys to the recovery of motor or sensory function after PNI. Li *et al.* loaded the peptides that could promote the adhesion of nerve cells on the scaffold with the microgroove structure and nanofiber oriented composite morphology.<sup>86</sup> The expressions of myelination-related genes and proteins in the SCs were up-regulated, which contributed to myelin regeneration and thus functional recovery.

Due to the electrophysiological properties of peripheral nerves, electrostatically activated electrospun scaffolds contribute to peripheral nerve regeneration and functional recovery when used as a bridge between the proximal and distal stump. Conductivity can be endowed to the conduits by coating the surface of electrospun fibers with conductive materials such as GO, reduced GO, polypyrrole, *etc.*<sup>87,88</sup> Wang *et al.* combined external electrical stimulation with reduced GO-modified NGC to promote the expression of genes related to remyelination in SCs.<sup>88</sup> The *in vivo* tests showed that the conduit group and the autograft group had similar myelin sheath thickness, axon diameter, nerve conduction velocity, and motor ability. Smaller self-powered NGCs are more attractive and convenient in peripheral nerve regeneration. As shown in Fig. 3C, a biodegradable electroactive conduit was fabricated by embedding a galvanic cell consisting of Mg and Fe–Mn alloy electrodes within a fibrous scaffold.<sup>89</sup> After implantation of the NGC to repair sciatic nerve injury in rats, the thickness of the regenerated myelin sheath and the recovery of motor function were comparable to those of the autograft group.

Although electrospun fiber-based NGCs have achieved similar repair effects to autografts in PNI less than 3 cm,<sup>66</sup> the results for repairing larger gap nerve defects are not satisfactory. Comprehensively integrating topological cues, biochemical cues, and exogenous cells into NGCs is promising to break down barriers to clinical treatment. Meanwhile, the availability and possibility of clinical translation is also a crucial factor to be considered. In addition, real-time monitoring of the regeneration process using modern imaging techniques and combining electrospun fibers with appropriate post-operative interventions, such as electrical stimulation, magnetic stimulation, optical stimulation, acoustic stimulation, and thermal stimulation, may further improve the effects of nerve regeneration.<sup>90</sup>

### 3.2 Central nerve regeneration

The central nervous system (CNS) consists of the brain and the spinal cord, which is the most principal part of the human nervous system.<sup>91</sup> The brain is located in the cranial cavity and mainly includes the left and right cerebral hemispheres. The superficial layer of the cerebral hemispheres is the gray matter, and the deep layer is the medulla, making up the organ that regulates the functions of the body and serves as the basis for higher neural activity.<sup>92</sup> The spinal cord is located in the spinal canal, with white matter in the center and gray matter in the periphery. The dorsal part of the spinal cord develops from the pterygoid plates of the neural tube during the embryonic period

and has mainly conduction functions. The ventral portion of the spinal cord develops from the substrate and has primarily reflex functions.<sup>93</sup> When damage to the CNS occurs, it can lead to a loss of motor function and sensation, causing severe life and psychological disorders to the patients. Central nerve injury has a high rate of disability, mortality, and complications, and is a major medical issue that needs to be addressed.<sup>94</sup>

Unlike PNI, the central nerve cannot regenerate itself, and CNS injury is often difficult to repair without the external intervention. Therefore, tissue regeneration scaffolds are usually required to facilitate the repair of CNS injury. The main obstacles to the repair of CNS injury include the deterioration of the ECM microenvironment due to inflammatory response, inadequate neurotrophic supply, and limited neuronal regeneration capacity.<sup>95</sup> To address these challenges, the bionic design of electrospun nanofiber scaffolds that can inhibit inflammation, provide neurotrophs, and regulate the directional differentiation of stem cells to neurons represents an important way to address the barriers to central nerve regeneration.

**3.2.1 Eliminate inflammation and inhibit gliosis.** Spinal cord injury (SCI) can be divided into primary SCI and secondary SCI. Primary SCI are mostly caused by mechanical impact.<sup>96</sup> While secondary injuries are triggered by the primary injury. After SCI occurs, macrophages are activated, and large amounts of proinflammatory factors, chemokines, NO, oxidants, and proteases can be released.<sup>97</sup> Erythrocytes enter the spinal cord parenchyma from the ruptured vessels, activating the macrophages into the M1 proinflammatory phenotype. The inflammatory microenvironment limits the differentiation of endogenous NSCs to neurons and instead promotes their differentiation to astrocytes. However, astrocytes are responsible for the formation of glial scars that impede axonal regeneration, severely hampering the repair of SCI. Therefore, suppressing the inflammatory response in the early stages of SCI is an important therapeutic strategy.

By introducing anti-inflammatory agents or biomolecules into electrospun nanofiber scaffolds, the inflammatory response can be effectively relieved. For example, researchers synthesized a polycarbonate with 17 $\beta$ -estradiol (E2) as one of the repeating units in the copolymer backbone.<sup>98</sup> E2 could reduce inflammation, decrease glial reactivity and oxidative stress, and reduce glutamatergic excitatory neuronal death. They subsequently prepared poly(pro-E2) electrospun nanofiber scaffolds.<sup>99</sup> The scaffold was able to release E2 over a period of 1–10 years after hydrolytic degradation *in vitro*. *In vivo* tests showed that the scaffold was able to effectively reduce the inflammatory response and guide axons along the aligned nanofibers for directed regeneration.

Neuroinflammation also severely affects the repair of brain injury. After secondary brain injury occurs, the blood–brain barrier is disrupted.<sup>100</sup> Microglia are activated, from which cytokines are released that activate other immune cells, initiating an inflammatory cascade at the site of injury, leading to neuroinflammation.<sup>101</sup> As microglia accumulate at the site of lesion, astrocytes are activated and thus form a glial scar. Therefore, suppression of neuroinflammation is also critical for brain

injury repair. Functionalized electrospun nanofiber scaffolds have great potential to eliminate inflammation. In one study, a novel galactose-presenting polymer, poly(L-lysine)-lactic acid (PLL-LBA), was synthesized.<sup>102</sup> Its layer-by-layer (LbL) functionalization of PCL nanofibers was achieved by covalently attaching galactose molecules to the surface of the nanofiber scaffold (Fig. 4A). Increased astrocyte GFAP expression and hypertrophy were the most

common hallmarks of reactive astrocyte proliferation. *In vitro* tests showed that the nanofiber scaffold significantly reduced GFAP expression, attenuated inflammation-induced astrocyte proliferation, and suppressed the adverse effects of the inflammatory response. Given the specific nature of brain injury, instead of defects or transection, cavities of unknown size and shape are often formed in the brain. Therefore, the development of injectable fibers capable

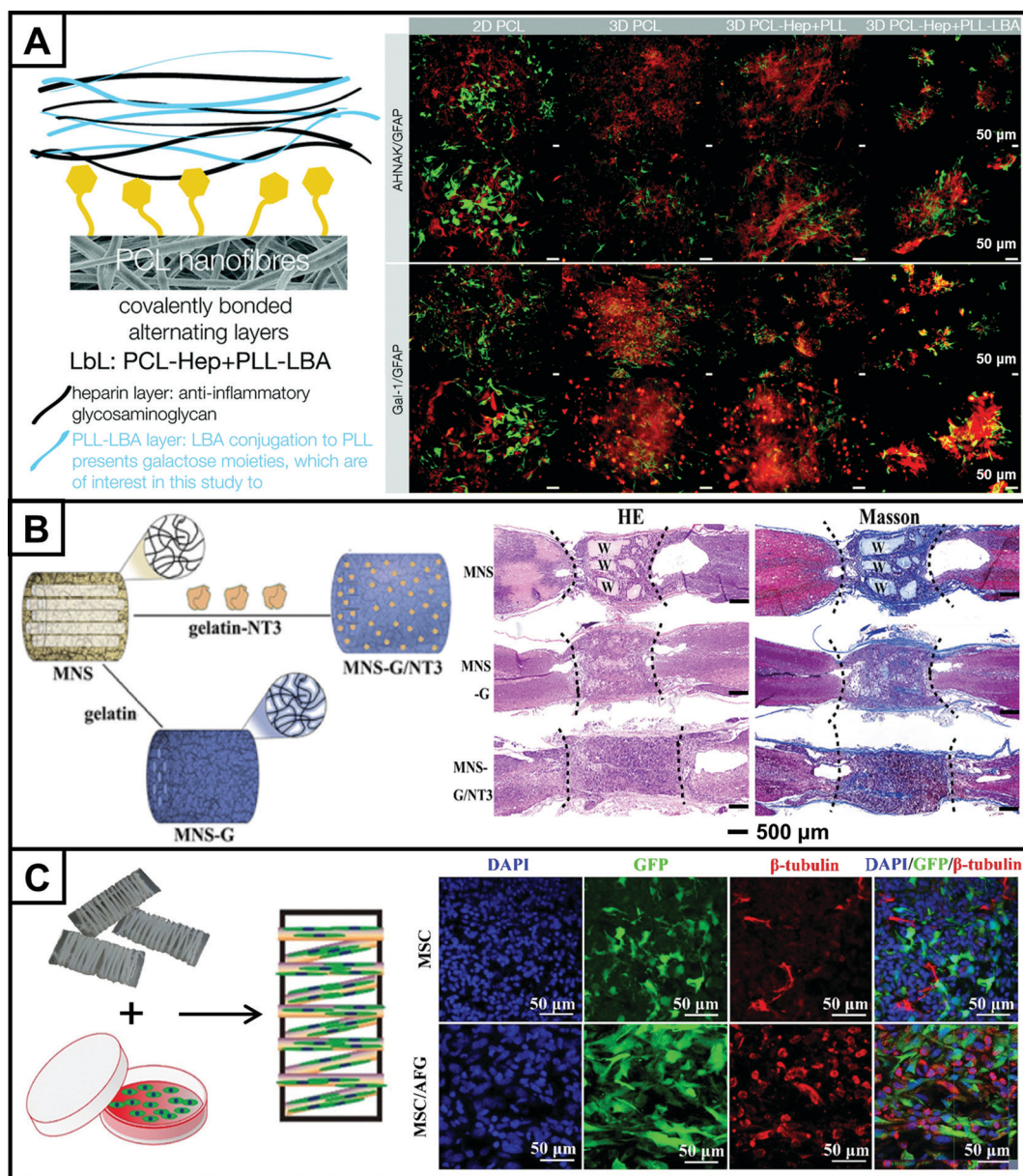


**Fig. 4** Electrospun nanofiber scaffolds for CNS injury repair. (A) Schematic representation of galactose molecules covalently attached to the surface of a nanofibrous scaffold (left). Fluorescence micrographs (right) showing AHNAK (red)/GFAP (green) and Gal-1(red)/GFAP (green) staining of astrocytes grown on 2D PCL, 3D PCL, PCL-Heparin (Hep) + PLL and PCL-Hep + PLL-LA at 12 div. (B) Schematic diagram illustrating the fabrication of gelatin-coated multichannel nanofiber scaffolds (MNS-G) loaded with NT-3 (MNS: multichannel nanofiber scaffolds) (left) and H&E and Masson staining images of the injury recovery, respectively, 8 weeks post-implantation. "W" denotes the side wall fragments of the nanofiber scaffolds (right). (C) Schematic illustration showing the aligned microfibrin hydrogel fibers (AFG) that were used as the carrier of MSCs to maintain the MSC-oriented adhesion (left), and typical CLSM images of MSC and MSC/AFG groups at the SCI site: blue is to label the nucleus, green is GFP to show the implanted MSCs, and red is the  $\beta$ -tubulin III-positive. All of them are merged to show the implanted MSC differentiation (right). (A–C) Reprinted with permission from ref. 102: Copyright (2017) The Royal Society of Chemistry, ref. 106: Copyright (2020) American Chemical Society, ref. 116: Copyright (2020) American Chemical Society, respectively.

of satisfactorily filling any cavity is crucial for the clinical management of brain injury. In another study, the researchers developed injectable and gel-like fibers.<sup>103</sup> The electrospun fibers were combined with a lubricated hydrogel to produce rheological properties that allowed them to maintain the basic morphology of the fibers after injection. Loading the fibers with hNSCs successfully blocked the infiltration of microglia in the inflammatory response in an MCAO model.

**3.2.2 Provide neurotropy.** After CNS injury occurs, NSCs around the injury are activated and begin to migrate toward the site of the injury. Since neurons in the CNS cannot regenerate after disruption or death, differentiation through NSCs is the only way for neuronal regeneration.<sup>104</sup> However, the proliferation and differentiation of NSCs are mainly influenced by the microenvironment of the ECM. After the occurrence of CNS injury, the supply of neurotrophic factors appears to be inadequate, causing severe damage to the microenvironment and inhibiting neural regeneration. Neurotrophic factors, such as ciliary neurotrophic factor (CNTF), BDNF, NT-3, and glial cell-derived neurotrophic factor (GDNF), play an important nutritional role in the growth, development, and functional integrity of neurons. Since neurotrophic factors protect neurons and repair damaged nerve cells, the deficiency of neurotrophic factors can lead to impaired central nerve regeneration. Providing exogenous neurotrophic factors through an electrospun nanofiber scaffold as a controlled delivery system is expected to supplement the deficiency of endogenous factors, improve the neuroregenerative microenvironment, and provide good conditions for the proliferation and differentiation of NSCs to neurons.

For the repair of SCI, a three-dimensionally aligned poly( $\epsilon$ -caprolactone-ethyl phosphate) (PCLEEP) electrospun nanofiber-collagen hybrid hydrogel was prepared.<sup>105</sup> The scaffold was loaded with NT-3 and miR-222, in which miR-222 is a microRNA that is enriched in axons and involved in controlling local protein synthesis in distal axons. Through the controlled delivery of the two biological effectors, the scaffold effectively improved the microenvironment of SCI and promoted the regeneration of nerve axons. In another study, poly(L-lactic acid) (PLLA) multichannel nanofiber scaffolds (MNS-G) were modified by gelatin and cross-linked with genipin (Fig. 4B).<sup>106</sup> The gelatin-coated nanofibers showed a strong binding affinity to NT-3, enabling the *in vivo* delivery and controlled release of NT-3. H&E staining showed a significant reduction in SCI cavities and tighter binding to the host in the presence of the scaffold because it provided a bionic environment and sufficient NT-3 for SCI, as well as promoted post-surgery neuronal regeneration and remyelination. This study demonstrated the easy modification of nanofiber scaffolds, which played an important role in guiding the design of repair scaffolds for SCI.

The supplementation of neurotrophic factors is also important after brain injury. In addition to their universal role in the CNS as described above, neurotrophic factors play an important role in the protection and functional recovery after neurodegenerative diseases such as stroke and traumatic brain injury. However, the supplementation with exogenous neurotrophic factors can be limited by the blood-brain barrier,

leading to the difficulty in reaching the target site. Therefore, *in situ* delivery of neurotrophic factors *via* electrospun nanofiber scaffolds is essential for microenvironmental repair of brain injury. In one study, a PCL nanofiber scaffold encapsulated with GDNF was prepared.<sup>107</sup> The scaffold had an oriented topology that could provide topographical cues to guide the behavior of NSCs. In addition, sustained release of GDNF was possible over one month, and the released GDNF significantly promoted the extension of neural axons. Electrospun nanofibers are not only capable of delivering neurotrophic factors, but also can immobilize the factors in a variety of ways.<sup>108</sup> Neurotrophic factors can be loaded into the nanofibers or deposited onto the nanofibers. When they are loaded into the nanofibers, neurotrophic factors are released in a sustained manner through nanofiber degradation and act on the site of injury over time. When they are deposited onto the nanofibers, they provide biochemical cues for NSC migration and differentiation, as well as axonal extension, in addition to delivery, and promote neuronal regeneration. Besides, by preparing stimulus-responsive nanofiber scaffolds, neurotrophic factors can also achieve controlled release triggered by the internal microenvironment or exogenous stimuli such as light, electricity, and magnetic field.<sup>109</sup> Therefore, electrospun nanofiber scaffolds have significant advantages in the supply of neurotrophic factors.

**3.2.3 Neuronal differentiation.** In the CNS, injured/diseased tissue typically undergoes liquefaction necrosis, where enzymes digest cellular debris and the ECM, usually leaving a fluid-filled cavity.<sup>110</sup> The neuronal cells at the site of injury become inactivated, leading to the destruction of neural networks and consequent dysfunction.<sup>111</sup> Due to the lack of growth-driven signals and subcellular structural arrangements, neuronal regeneration in the adult CNS capacity is low. Therefore, inducing NSCs to differentiate into neurons rather than glial cells is essential to improve the regeneration efficiency of CNS injury. Given these characteristics, it is necessary to use the scaffolds to (i) immobilize endogenous or transplanted cells, (ii) protect endogenous or transplanted cells from the effects of injury, and (iii) regulate the differentiation of endogenous or transplanted cells. Functional electrospun nanofiber scaffolds have shown efficiency in mitigating the effects of poor SCI microenvironment and promoting neuronal differentiation of stem cells.<sup>112</sup>

Endogenous NSCs are derived from ectodermal cells of the central canal of the adult spinal cord, which have multiple differentiation potential.<sup>113</sup> These cells can be induced to proliferate and differentiate into astrocytes, oligodendrocytes, and neurons in response to stimulation by injury, which can serve as an internal cell source for central nerve repair. In one study, an elastic low-modulus bionic scaffold was constructed using electrospun GelMA hydrogel nanofibers to provide a favorable microenvironment for nerve repair and regeneration.<sup>114</sup> The scaffold could promote the migration of endogenous NSCs and induce their differentiation into neuronal cells to promote SCI repair. Bio-functional scaffolds capable of supporting neurite growth, guiding neurite extension, and reconstructing damaged brain tissue are also urgently needed for the repair of brain injury.

To this end, aligned electrospun poly(lactic-co-glycolic acid) (PLGA) nanofibers were prepared and functionalized with hydrolyzed monosialic acid ganglioside (LysoGM1).<sup>115</sup> The addition of LysoGM1 conferred bioactivity to the nanofiber scaffold to promote neuronal membrane formation. In a rat TBI model, the aligned PLGA-LysoGM1 nanofiber scaffold promoted neurite growth and infiltration, showing great potential in brain tissue regeneration.

In addition to promoting CNS regeneration by modulating endogenous cells, it is also possible to promote CNS regeneration by delivering exogenous stem cells and modulating their directed differentiation into neurons. Exogenous stem cells capable of differentiating into neurons include embryonic stem cells (ESCs), neural progenitor cells, olfactory ensheathing cells (OECs), adult MSCs, NSCs, *etc.* Stem cell therapy is widely recognized as a promising approach to reconstruct the structure and function of the CNS. The delivery of stem cells through electrospun nanofiber scaffolds can overcome the disadvantages of clinical stem cell transplantation therapies. In one study, aligned electrospun fibrin hydrogel nanofibers loaded with MSCs were prepared (Fig. 4C).<sup>116</sup> MSCs fused well with the host tissue by adhesion and induction of nanofibers. The staining results demonstrated the ability of the scaffold to induce the differentiation of MSCs into neurons, as well as to promote the migration and aggregation of endogenous neurons and MSC-differentiated neurons toward the injury site. The scaffold promoted the expression of electrophysiology in the spinal cord by regulating the migration and differentiation of MSCs, which in turn facilitated the recovery of spinal cord function. In another study, an artificial 3D electroactive neural network system was constructed by loading brain neural progenitor cells into a high-porosity, low-density electrospun PCL nanofiber scaffold.<sup>117</sup> The network promoted neuronal differentiation and growth and further promoted the formation of functional synapses. The nanofiber scaffold combined electroactivity and cell delivery, playing an important role in the regeneration of brain tissue and restoration of brain function.

In the CNS, electrospun nanofibers have great appeal due to their bionic structural features, compositional diversity, easy modification, and deliverability. However, there are not many studies on the application of nanofibers for CNS injury repair, and one of the reasons is that the implantation of electrospun nanofiber scaffolds often requires an open surgery.<sup>118</sup> Given the advantages of electrospun nanofibers, injectable treatments can be achieved by preparing short nanofibers.<sup>119</sup> In addition, electrospun nanofibers can be combined with imaging agents to achieve a real-time monitoring *in vivo* during and after surgery, guaranteeing a precise surgery and timely repair process to achieve integration of monitoring and treatment.<sup>120</sup> The advanced electrospun nanofibers will hopefully solve the major challenges of central nerve injury, effectively bringing hope to the lives of brain injury and spinal cord injury patients worldwide and helping them to return to society.

### 3.3 Skin regeneration

As the largest organ of the body, the skin is a barrier that separates the body from the external environment.<sup>121</sup> Under normal physiological conditions, the skin protects the body

from chemicals and other harmful substances, UV radiation, and water loss.<sup>121,122</sup> However, when the structure of the skin is damaged, it can lead to impaired skin function and the formation of wounds. Mechanical trauma, burns, tumors, chronic diseases, and genetic disorders are the main causes of wounds.<sup>123</sup> The “golden standard” in clinical treatment of skin wounds is autologous skin grafting.<sup>124</sup> However, the lack of skin donor sites, secondary damage, and risk of infection limit its application.<sup>125,126</sup> Therefore, the development of wound dressings that promote skin tissue regeneration is expected to address the shortcomings of autologous grafting, which is of great clinical importance.

Electrospinning has unique advantages in the preparation of wound dressings. As wound dressings, the porous structure of electrospun nanofiber scaffolds can enhance the adsorption of wound exudate and promote the exchange of oxygen, water, and nutrients.<sup>127,128</sup> In addition, electrospun nanofibers can provide topographical cues and biochemical cues for skin tissue regeneration through special structural and compositional design.<sup>129,130</sup> Combined with the controlled delivery of drugs or bioactive substances, the electrospun fibers can further achieve antibacterial and anti-infection effects, promote vascular regeneration, facilitate cell migration, and eventually realize scar-free skin wound healing.

**3.3.1 Antibacterial and anti-infection functions.** In open wounds, there is a high risk of bacterial invasion. Bacterial invasion into the lymphatics and blood can cause serious infections and even fatal sepsis.<sup>131,132</sup> Some bacteria also reduce the immune function of the body and impede wound healing by producing enzymes and toxins.<sup>133</sup> The current clinical treatment of infection is still dominated by antibiotics. However, the misuse of antibiotics can lead to drug resistance which poses a great danger to life and health.<sup>134</sup> The development of wound dressings with antibacterial properties can overcome the disadvantages of antibiotics and promote wound healing. The porous structure of electrospun fibers makes them inherently resistant to external bacterial invasion, and the introduction of antibacterial components allows them to further kill bacteria. An ideal antibacterial dressing can reduce the number of pathogens and reduce the inflammatory response of the wound, which in turn improves wound repair. Guo *et al.* synthesized quaternized chitosan-graft-polyaniline (QCSP), which exhibited better cytocompatibility and antibacterial activity than pure quaternized chitosan.<sup>135</sup> Electrospun PCL/QCSP nanofibers were then fabricated, which showed a good killing rate against both *Staphylococcus aureus* (*S. aureus*) and *Escherichia coli* (*E. coli*). The antibacterial activity gradually increased with the increase of the QCSP content in the dressing and showed a good therapeutic effect in wound healing.<sup>136</sup>

In addition to using antibacterial materials, antibacterial agents can be loaded inside or on the surface of electrospun fibers to impart them resistance to bacterial invasion. For example, polyoxyethylene and oxacillin were co-loaded in electrospun poly(lactic acid) (PLA) nanofibers to develop a multifunctional fiber dressing.<sup>137</sup> The sustained release of the two antibacterial agents synergistically inhibited methicillin-resistant *Staphylococcus aureus*. Furthermore, a layer of polyacrylonitrile (PAN) nanofibers

encapsulated with phenol red was overlaid on top of the PLA nanofiber membrane. Given that the pH of the infected wounds is higher than that of the normal skin, the detection of pH at the wound site can provide important information for wound repair and care. The presence of phenol red allowed the real-time monitoring of pH at the wound site. This combination of diagnosis, monitoring, and treatment is typically important for the regeneration of skin damage.

For multidrug-resistant (MDR) bacterial infections, the effectiveness of conventional antibacterial agents is often greatly reduced. Metal ions such as gold (Au) ions and silver

(Ag) ions have broad-spectrum antibacterial properties and are also involved in a variety of biological processes in the body. Therefore, metal ion-based wound repair platforms have immense potential in the treatment of wounds infected with bacteria.<sup>138,139</sup> Au nanoparticles are one of the few inorganic metal nanoparticles that can destroy both Gram-negative and Gram-positive bacteria while being effective against MDR infections.<sup>140,141</sup> In one study, AuNPs were modified with 6-aminopenicillic acid, an antimicrobial intermediate, and then incorporated as the active antibacterial component into electrospun PCL/gelatin fibers (Fig. 5A).<sup>142</sup> The scaffold was then

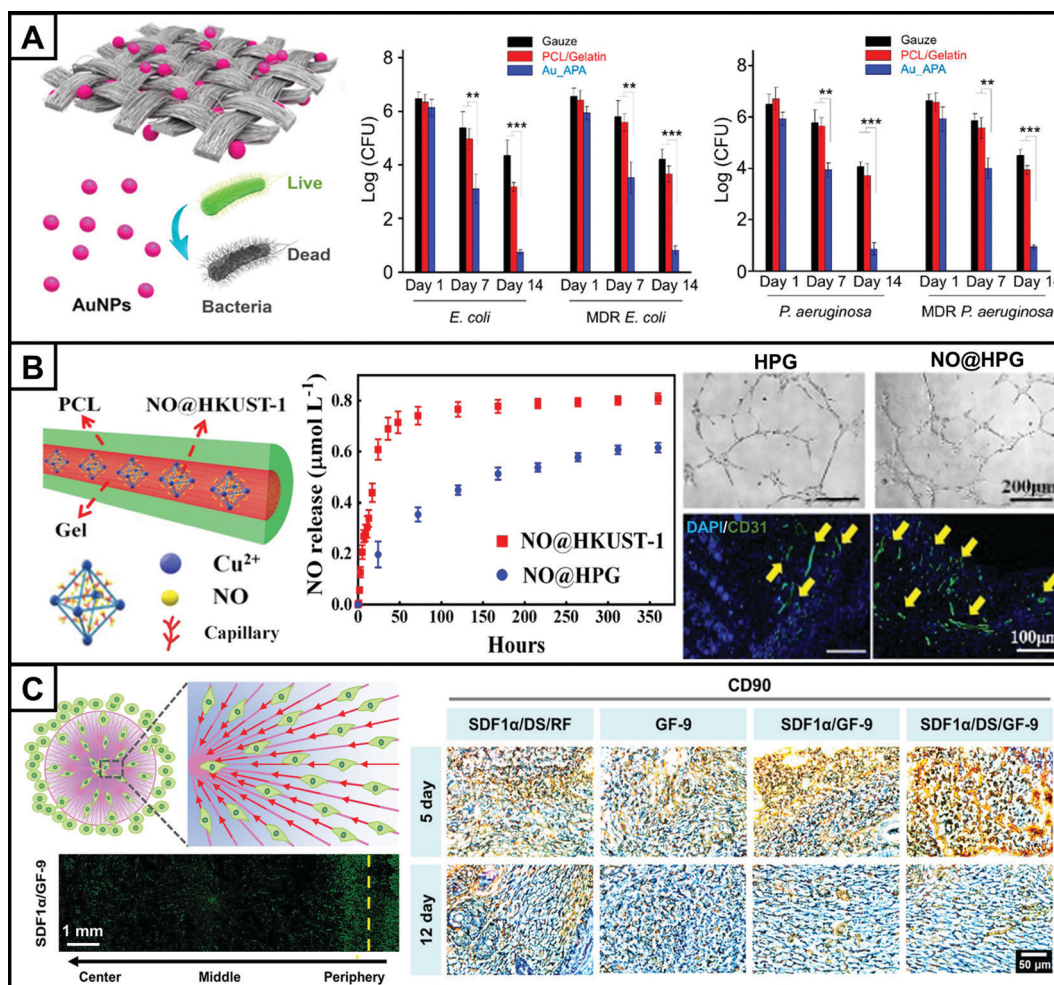


**Fig. 5** An electrospun nanofiber scaffold for skin tissue repair. (A) Schematic representation of a knitted dressing made of PCL/gelatin electrospun nanofibers doped with antimicrobial AuNPs (left). The gauze group, PCL/gelatin group, and APA-modified AuNPs (Au\_APA) group were used for treating wounds infected by *E. coli*, MDR *E. coli*, *Pseudomonas aeruginosa*, and MDR *Pseudomonas aeruginosa*, and bacterial counts at 7 and 14 days demonstrated the ability and effectiveness of the composited fibers to reduce local bacterial infections (right). (B) Schematic structure of the PCL-gelatin core-sheath fibers loaded with NO-containing copper MOF (NO@HKUST-1) nanoparticles (NO@HPG) (left). Cumulative release of NO from NO@HKUST-1 and NO@HPG in PBS (middle). Tube formation of HUVECs cultured with HPG and NO@HPG after culturing for 6 hours (upper right). Immunofluorescent staining (lower right) showing CD31 expression on HPG and NO@HPG at 7 days. The blood vessels were stained with CD31 (green), and the cell nuclei were stained with DAPI (blue). (C) Schematic representation and live/dead staining of MSCs cultured on the SDF-1 $\alpha$  gradient electrospun nanofiber scaffolds prepared using a collector with 9 needle electrodes (GF-9) after 7 days. The maximum migration distance of MSCs reached the center, demonstrating the induced promotion of MSC migration by SDF-1 $\alpha$ /GF-9 (lower left). Immunohistochemical staining using CD90, a classical MSC surface marker, was performed at 5 and 14 days in the damaged skin, with positive expression in brown and blue nuclei (right). Positive CD90 staining was significantly increased in the GF-9 group with both SDF-1 $\alpha$  gradient and encapsulated DS (SDF-1 $\alpha$ /DS/GF-9) compared to the other groups, demonstrating the effect of gradient release of SDF-1 $\alpha$  and reduction of inflammation on the recruitment of endogenous stem cells to the wound. (A–C) Reprinted with permission from ref. 142: Copyright (2017) American Chemical Society, ref. 151: Copyright (2020) American Chemical Society, and ref. 158: Copyright (2021) John Wiley and Sons, respectively.

applied to treat rat wounds exposed to *E. coli*, MDR *E. coli*, *Pseudomonas aeruginosa*, and MDR *Pseudomonas aeruginosa*, respectively, for 14 days, indicating that both local bacteria and MDR bacteria were significantly reduced in comparison to the PCL/gelatin and gauze groups. This work demonstrated the effectiveness of bioactive electrospun fiber scaffolds in dealing with MDR bacterial infections, which went beyond traditional antibacterial agents to address the problem of MDR bacterial infection, indicating the potential of metal ion-containing antibacterial dressings for wound repair applications.

**3.3.2 Angiogenesis.** The skin is a highly vascularized soft tissue;<sup>143</sup> therefore, angiogenesis after skin injury is essential for skin regeneration. Angiogenesis is the hallmark of the proliferative stage, so accelerated angiogenesis will promote wound repair and shorten healing time, as well as effectively prevent necrosis.<sup>144–146</sup> Conversely, a poor angiogenesis can lead to delayed wound closure, increase the risk of infection, and pose a significant challenge to wound healing,<sup>147</sup> in particular for chronic wounds caused by diabetes that often suffer from insufficient angiogenesis and delayed healing.

Loading angiogenesis-promoting drugs or growth factors into electrospun fiber dressings can improve angiogenesis and promote wound recovery. For example, tazarotene, an active drug that promotes angiogenesis, was loaded into aligned PCL fibers.<sup>148</sup> The sustained release of tazarotene from the nanofibers stimulated the proliferation, migration, and vascularization of human umbilical vein endothelial cells (HUVECs) and promoted the secretion of VEGF. *In vivo* tests showed that the tazarotene loaded fibers significantly improved angiogenesis, promoted re-epithelialization, and accelerated wound healing. The type, release profile, and bioactivity of the drugs need to be considered for promoting angiogenesis.

In addition to active drugs, some growth factors are closely related to angiogenesis. Skin regeneration is a complex process that involves the interaction of multiple growth factors in various processes. Among them, VEGF is the most important growth factor involved in the angiogenesis process. Other growth factors essential for angiogenesis include platelet-derived growth factor (PDGF), fibroblast growth factor (FGF), insulin growth factor (IGF), hepatocyte growth factor (HGF), and stromal cell-derived growth factor (SDF). The introduction of growth factors into electrospun fibers can complement endogenous growth factors and provide the necessary conditions for angiogenesis. In one study, core–sheath electrospun fibers were prepared by coaxial electrospinning, with the core layer being made of polyethylene oxide (PEO) and recombinant human-VEGF (rhVEGF) and the shell layer being made of polycaprolactone and polyethylene glycol (PEG).<sup>149</sup> It showed that the rhVEGF was able to achieve a continuous release for 18 hours. In a mouse subcutaneous model, fibers loaded with rhVEGF significantly enhanced the formation of blood vessels. In another study, VEGF-encapsulated gelatin particles were loaded into electrospun PCL nanofibers.<sup>58</sup> VEGF could diffuse out of the PCL nanofibers through gelatin degradation and was released at the injury site. The results indicated that the scaffold could differentiate MSCs to ECs while maintaining the tubular

structure stability of ECs for a prolonged duration. Related designs can be integrated in the fiber-based dressing system to improve the utilization efficiency of bioactive molecules and further improve the regeneration efficacy.

The angiogenesis process can also be regulated by typical types of molecules. For example, NO plays an important role in wound healing by promoting angiogenesis and is an important cell signaling molecule.<sup>150</sup> Delivery of an appropriate concentration of NO to the wound site can inhibit apoptosis, promote cell proliferation and angiogenesis, and thus facilitate wound repair. Therefore, achieving a controlled release of NO and maintaining the ideal concentration is the key to NO treatment for skin injury. In one study, a copper-based metal–organic framework was applied as the carrier of NO which was then loaded into the core layer of electrospun PCL/gelatin core–sheath nanofibers by coaxial electrospinning (Fig. 5B).<sup>151</sup> The exudate from the wound entered the fibers and underwent a water replacement reaction in contact with the nanoparticles, allowing the release of NO and copper ions ( $\text{Cu}^{2+}$ ). Furthermore, NO and  $\text{Cu}^{2+}$  were released from the core layer through degradation. As a result, a stable and sustained release of NO and  $\text{Cu}^{2+}$  was achieved, which could last for more than 14 days. The composite fiber scaffold significantly promoted tube formation of HUVECs *in vitro* and CD31 expression *in vivo* compared to the fibers without NO, demonstrating the role of NO in angiogenesis.

In addition to the abovementioned active ingredients such as drugs, growth factors, and the gas NO, bioactive glass and bioceramics are also materials with unique characteristics for biomedical applications, especially for angiogenesis. Bioactive glasses are a class of materials that can repair, replace, or regenerate injured tissues, and have the ability to form bonds between tissues and materials. Bioactive elements such as Ag, Ca, Co, Cu, Ga, Mg, and Zn can be incorporated into the glass network to confer biofunctionality to the material. In skin tissue regeneration, bioactive glasses and their released therapeutic ions can promote fibroblasts to secrete vascular-derived growth factors such as VEGF and bFGF, and induce endothelial cells to migrate to the wound site, improving the insufficient angiogenesis at the wound center.<sup>152</sup> In addition, bioceramics are also materials with significant potential to promote vascular regeneration. Bioceramics are a class of ceramic materials used for specific biological or physiological functions, including hydroxyapatite, silica, calcium phosphate, *etc.* For example, silica-loaded-PCL electrospun nanofibers have been studied to accelerate angiogenesis by promoting endothelial cell adhesion, elongation, and migration.<sup>153</sup>

**3.3.3 Migration of repairable cells.** After the appearance of the wound, the cells around the wound begin to proliferate and migrate toward the center of the injury. As a result, fibroblasts eventually form granulation tissue, basal cells form a single layer of epithelium covering the surface of the granulation tissue, and keratinocytes form an epidermis located in the outermost layer of the skin, which becomes a keratinized complex squamous epithelium.<sup>154,155</sup> The integrity of the skin is the basis for the restoration of the complete barrier function of the skin. During the process of wound repair, cell proliferation is

relatively easy to be achieved, and cell migration can be relatively difficult, especially in chronic wounds. Therefore, promoting cell migration through electrospun fiber scaffolds is crucial for skin regeneration.

The composition of the fibers can affect cell behaviors. As a typical example, chitosan has been reported to induce the release of interleukins associated with migration and proliferation from fibroblasts, accelerating granulation tissue formation by promoting the migration of fibroblasts to the wound center, thereby promoting skin regeneration.<sup>156</sup> A PCL/chitosan core-sheath scaffold fabricated by emulsion electrospinning could significantly promote cell adhesion, migration, and proliferation, and further promote the healing of full-thickness skin injury in rats.<sup>157</sup>

The surface topography of electrospun fibers also has an impact on cell migration. Compared to random nanofibers, aligned nanofibers can provide topographic cues for cell migration, thus guiding cells to converge in the direction of fiber orientation. In addition, active substances with gradient density can be deposited on the fiber surface. The gradient of the active substance can provide biochemical cues for cell migration, inducing cells to migrate in the direction of increasing gradient. The combination of topographical cues and biochemical cues can synergistically promote cell migration and thus accelerate wound healing. Du *et al.* designed a radially assembled PCL/collagen electrospun nanofiber scaffold encapsulated with the anti-inflammatory agent, diclofenac sodium.<sup>158</sup> A gradient of SDF-1 $\alpha$  increasing from the periphery to the center was also constructed on the surface (Fig. 5C). SDF-1 $\alpha$  is a repellent factor that directs stem cell migration and regulates their behaviors by specifically binding to receptors on the surface of stem cells.<sup>159</sup> The radial topography combined with the gradient of SDF-1 $\alpha$  promoted the migration of MSCs. *In vivo* tests demonstrated that the scaffold promoted the migration of endogenous stem cells to the wound center and accelerated skin regeneration.

It remains an important issue to achieve the controlled release of bioactive substances loaded in electrospun fiber scaffolds. The controlled release can be triggered by external stimuli such as light, heat, electrical and magnetic fields, and even mechanical change. In one study, a multilayered photothermal scaffold was constructed by combining electrospun fiber scaffolds with NIR light and a tunable photomask.<sup>39</sup> The inner layer of the scaffold was composed of radially aligned nanofibers, while the outer layer was composed of random nanofibers. The PCM microparticles with a core layer of EGF were sandwiched between the two layers of nanofibers. A size-tunable photomask was placed between the scaffold and the NIR light source, and the PCM microparticles in the scaffold exposed to the NIR light warmed up and underwent solid-liquid transformation, leading to the triggered release of EGF. As the diameter of the photomask was decreased, EGF was sequentially released from the typical position of the scaffold exposed to the laser, from the periphery to the center, promoting the migration of fibroblasts along the radial direction. The introduction of the NIR light achieved a time-controlled release. By changing the position and size of the photomask,

a location-controlled release was achieved. Thus, the scaffold realized a spatiotemporally controlled release of growth factors, which in combination with the radially aligned topology greatly facilitated cell migration. The scaffold showed great potential for application in wound repair. Skin regeneration is a complex process involving several overlapping stages. Designing scaffolds that meet the needs of each stage and achieve multifunctional integration remains an important research direction. This requires the integration of multiple factors. Based on the existing research, combining topographical and biochemical cues with controlled release and exogenous stimulation to further improve the scaffolds will facilitate the application of electrospun fiber scaffolds in skin regeneration.

### 3.4 Cardiac tissue regeneration

The heart is a muscular organ with a complex structure and biological function. The human heart is in the middle of the thoracic cavity and has four internal cavities, the upper two being the atria and the lower two being the ventricles. The diastole and contraction of the atria and ventricles drives blood throughout the body, providing oxygen and nutrients to organs and tissues.<sup>160</sup> Cardiovascular diseases such as myocardial infarction, heart failure, and coronary artery disease caused by ischemia and hypoxia, dysfunction, and cardiac degeneration are threatening the lives of tens of millions of patients worldwide.<sup>161</sup> Common clinical treatments include coronary artery bypass grafting, heart transplantation, and stenting. However, due to the limited regenerative capacity of the heart, the existing treatments can only temporarily maintain heart function and cannot restore normal heart function. There are also disadvantages such as heart size mismatch, vascular lesions, and shortage of supply.<sup>162</sup> Therefore, the development of scaffolds for application in cardiac tissue regeneration is expected to address these deficiencies, which are of great clinical importance.

Electrospun nanofibers have unique advantages as cardiac repair scaffolds. Aligned nanofibers with a significantly high surface-to-volume ratio and porosity can guide the ordered arrangement of fibroblasts and promote the adhesion and maturation of cardiomyocytes.<sup>163,164</sup> Meanwhile, electrically conductive aligned scaffolds can facilitate muscle contraction and synchronized electrical conduction, thus enabling synchronized beating of cardiomyocytes.<sup>165</sup> With proper structural design and the combination of drugs or bioactive factors, electrospun nanofibers can further inhibit fibrosis and adverse cardiac remodeling, as well as achieve the effect of myocardial endothelialization.

#### 3.4.1 Anti-fibrotic and anti-adverse ventricular remodeling.

When myocardial infarction episodes, cardiomyocytes are damaged and necrosis occurs due to ischemia and hypoxia, generating large amounts of reactive oxygen species (ROS) in the microenvironment.<sup>166</sup> The production of ROS causes oxidative stress, disrupts cellular homeostasis, leads to further apoptosis, and promotes inflammatory response and fibrosis.<sup>167,168</sup> Excessive inflammation in turn promotes the production of ROS, creating a fibrotic microenvironment that leads to collagen



deposition and eventual ventricular remodeling.<sup>169</sup> This usually leads to chronic irreversible heart failure and even death.<sup>170</sup> Therefore, reducing inflammation in the early stages of myocardial infarction is beneficial in preventing myocardial cell damage, reducing adverse fibrosis, inhibiting ventricular remodeling and scar tissue formation, and promoting angiogenesis in the lesion area.<sup>171</sup>

Reducing ROS levels in damaged myocardial tissues is an effective strategy to reduce inflammation, avoid fibrosis, and inhibit ventricular remodeling.<sup>172</sup> Therefore, the preparation of biological scaffolds with good antioxidant properties that can respond rapidly to ROS will be beneficial for myocardial repair.<sup>173</sup> Xie *et al.* synthesized one type of polyurethane (PFTU) from several polymers rich in thioketone bonds to take advantage of the thioketone bonds for reacting and decomposing ROS.<sup>174,175</sup> Then, a cardiac patch based on PFTU/gelatin nanofibers was fabricated by electrospinning. *In vitro* tests demonstrated that the nanofiber patch showed good antioxidant activity and could rapidly respond to and degrade ROS while alleviating oxidative stress. Transplantation of the patch into rats effectively alleviated oxidative damage and suppressed the inflammatory response in the early stages of myocardial infarction. In addition, left ventricular remodeling was also inhibited by the nanofiber patch, thus enhancing the effect of later myocardial repair. The patch had good antioxidant properties and rapid ROS scavenging ability, making it an effective method for anti-fibrotic and reversible ventricular remodeling.

In addition to the use of antioxidant materials, loading anti-inflammatory agents or bioactive regulators into electrospun nanofibers can also achieve anti-inflammation and antifibrosis functions. Glucocorticoid methylprednisolone (MP) is an anti-inflammatory drug commonly used in the treatment of myocardial infarction, which can effectively modulate the inflammatory response.<sup>171</sup> In one study, researchers prepared electrospun polyurethane (PUTK) nanofiber patches loaded with MP.<sup>176</sup> Although the PUTK fibers themselves had antioxidant properties, the addition of MP conferred a higher ROS responsiveness. Besides, PUTK/MP fibers could restore cardiac function better than PUTK fibers, significantly reducing fibrosis and adverse ventricular remodeling. Angiotensin-converting enzyme 2 (ACE2) is a novel bioactive regulator, and its over-expression within the heart can reduce myocardial fibrosis, mitigate oxidative damage, and restore cardiac function.<sup>177</sup> For example, a hyaluronic acid (HA)-PLLA core-sheath nanofiber cardiac patch with a core layer loaded with rhACE2 was obtained by microsol electrospinning (Fig. 6A).<sup>178</sup> In a rat model of myocardial infarction, the sustained release of rhACE2 attenuated fibrosis and counteracted unfavorable ventricular remodeling, maintaining normal ventricular structure and function, thus demonstrating the potential of rhACE2 in cardiac tissue regeneration.

**3.4.2 Adhesion, maturation, and synchronized beating of cardiomyocytes.** The native myocardium in the human body is composed of several layers of longitudinally aligned and neatly packed cardiomyocytes, which control the mechanical contraction of the heart through their synchronized beating.<sup>179</sup>

Cardiomyocytes regulate gene expression, protein synthesis, and other signals of cardiac function through mechanotransduction.<sup>180</sup> When myocardial infarction occurs, cardiomyocytes undergo apoptosis, the anisotropic cell structure is destroyed, the heart beats abnormally, and cardiac function is impaired.<sup>181</sup> The damaged myocardial tissue is unable to repair itself and therefore requires a cardiac tissue regeneration scaffold to promote myocardial regeneration.<sup>182</sup> Modulating the morphology and structure of electrospun nanofiber scaffolds can endow them with functions that promote the adhesion and maturation of cardiomyocytes. In addition, the electrospun nanofiber scaffolds have good mechanical properties, which can ensure the synchronized beating of cardiomyocytes and realize the regular contraction of the heart.

The surface topography of electrospun nanofiber patches can provide topographical cues to the migration and morphology of cardiomyocytes.<sup>165</sup> In one study, an electrospun nanofiber patch made of polyvinylidene fluoride-trifluoroethylene (PVDF-TrFE) copolymer was developed.<sup>183</sup> *In vitro* tests showed that cardiomyocytes migrated along the PVDF-TrFE nanofibers in the direction of orientation and self-assembled into elongated and aligned tissues. Piezoelectric phenomena showed a regular contraction of the heart, demonstrating synchronized beating of the cardiomyocytes. In another study, an aligned PCL electrospun nanofiber patch was fabricated and then cultured with cardiomyocytes differentiated from human iPSCs.<sup>184</sup> Compared with those on a random PCL nanofiber patch, the cells cultured on the aligned patch were highly oriented and showed higher maturation and contraction rates. In cardiac tissue regeneration, although nanofiber patches can be designed to guide the migration and tensile growth of cardiomyocytes along the axial direction, their role in promoting maturation and endothelialization of cardiomyocytes is still relatively limited.<sup>185</sup>

Compared with nanofiber patches, 3D nanofiber scaffolds can mimic the anisotropic structure of the heart and possess better mechanical properties. For example, researchers prepared electrospun PCL nanofiber mats with aligned fibers at the central part and random fibers at the periphery.<sup>186</sup> A 3D nanofiber scaffold was obtained by sequentially stacking three layers of nanofiber mats with different orientation directions at the central part. The scaffold had good mechanical stability and was able to promote the alignment, adhesion, and maturation of cardiomyocytes along the orientation direction of the nanofibers to form a specific layer of cells for initial endothelialization. Meanwhile, each layer of cardiomyocytes achieved not only uniaxial synchronous contraction throughout the monolayer, but also a multiaxial contraction in the major directions at the spatial level, confirming that the scaffold achieved cardiac anisotropy. The stereotactic structure of this scaffold was thin, with fewer oriented links, which could be further improved to promote myocardial endothelialization. Inspired by the arrangement of natural cardiomyocytes, Wu *et al.* weaved neatly arranged nanofiber yarns (NFYs) with surgical sutures (NETS) using a braiding technique to produce an electrospun nanofiber scaffold (NFYs-NETS) and then encapsulated the scaffold in a hydrogel matrix to obtain a 3D composite scaffold (Fig. 6B).<sup>187</sup>

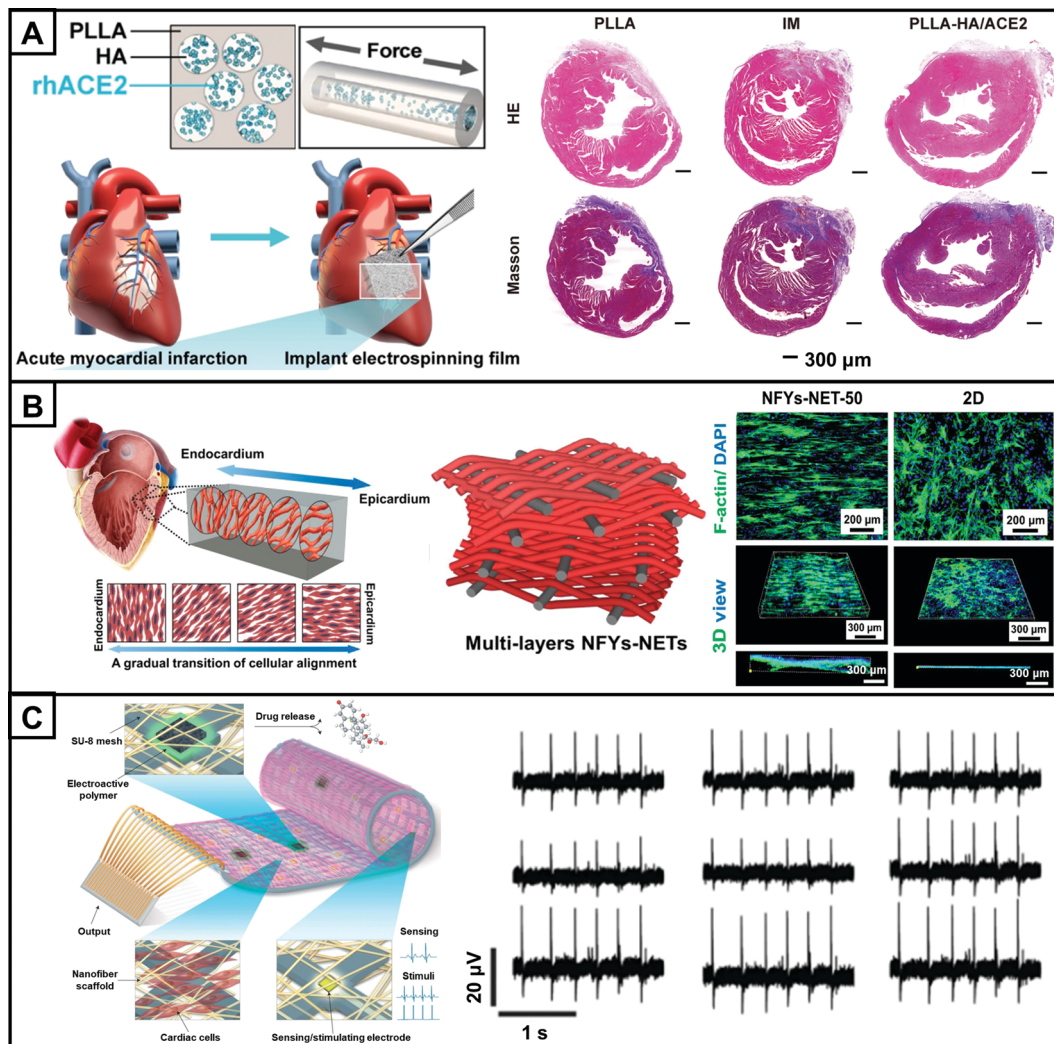


**Fig. 6** Application of electrospun nanofibers in cardiac tissue engineering. (A) Schematic diagram of the PLLA-HA/rhACE2 scaffold with the core–sheath structure fabricated by microsol electrospinning technology (upper left). Schematic diagram of the electrospun scaffolds implanted *in vivo* in a mouse myocardial infarction model (lower left). After 28 days of stent implantation, the heart sections of mice were subjected to H&E staining and Masson trichrome staining, the group containing rhACE2 showed significant differences in infarct scar expansion from the other groups, showing better preservation of the left ventricular structure (right). (B) Schematic diagram for natural heart tissue with cardiomyocytes uniformly arranged in each layer mid-up and gradually transitioning between layers (left). Schematic diagram of multilayer NFYs-NET 3D scaffold (middle). Fluorescence images show that cardiomyocytes are neatly aligned and evenly distributed on the surface of the NFYs-NET scaffold compared to the 2D scaffold, demonstrating the guiding effect of the 3D structure on cell adhesion migration. Cardiomyocytes were stained with F-actin (green) and DAPI (blue) (right). (C) Schematic diagram of an electrospun polycaprolactone-gel nanofiber patch incorporating a controllable electronic device (left). Cardiomyocyte electrophysiological data collected using nine electrodes on the electronic device demonstrate similar electrical signals, indicating synchronized beating of cardiomyocytes (right). (A–C) Reprinted with permission from ref. 178: Copyright (2021) Springer Nature, ref. 187: Copyright (2017) American Chemical Society, and ref. 191: Copyright (2016) Springer Nature, respectively.

Compared with the 2D scaffolds, the cultured cardiomyocytes on each layer of the 3D composite scaffold were not only neatly aligned and elongated but also had enhanced cell adhesion, viability, and maturation, and achieved myocardial endothelialization. To this end, 3D electrospun nanofiber scaffolds can provide a more bionic growth environment for cardiomyocytes, regulate cardiomyocyte behavior more effectively, and have great potential in cardiac tissue regeneration.

Furthermore, the synchronized beating of cardiomyocytes is a hallmark of electrical coupling in cardiac tissue.<sup>182</sup> Electrospun nanofiber scaffolds with electrical conductivity can mimic

the electrical signaling behavior of cardiomyocytes, thereby modulating the proliferation, differentiation, and migration of cardiomyocytes and enhancing the synchronized contraction of cardiomyocytes.<sup>188</sup> PANI is one of the widely used conductive polymers in biomedical applications. Wang *et al.* reported a PLA/PANI conductive electrospun nanofiber patch.<sup>189</sup> Cell proliferation of cardiomyocytes cultured on the PLA/PANI nanofiber patch was significantly enhanced, and the differentiation and maturation of CMs were significantly promoted. Furthermore, this PLA/PANI nanofiber patch with good electrical conductivity successfully induced spontaneous synchronous beating of

cardiomyocytes, demonstrating the role of the electrical activity of the material in promoting the electrical coupling of cardiomyocytes. To continuously monitor and control the patch after implantation in the body, remote manipulation of the electronic devices is needed and can be achieved by creating an electronic network together with the patches that enables the real-time monitoring and noninvasive interventional therapy *in vitro*.<sup>190</sup> Feiner *et al.* prepared an electronic device capable of effectively controlling drug release and integrated it with an electrospun PCL-Gel nanofiber patch for cardiac tissue regeneration (Fig. 6C).<sup>191</sup> This 3D tissue engineering scaffold was loaded with cardiac cells. By delivering functional cardiac cells, it was possible to provide therapeutic control and modulate cardiac function. In addition to the cardiac cells, electroactive polymers containing biomolecules were deposited at the electrode sites. Given that the nanofiber patch was a complex network containing multiple electrodes, the biomolecules were triggered to release by electrical stimulation while recording the behavior of cardiac cells *in vivo*. The patch prepared in this experiment realized controlled release and real-time monitoring, which had significant potential for patch intervention therapy. The results showed that cardiomyocytes on the patch produced a regular shape with consistent width and a consistent electrical signal, showing the synchronized beating of the cardiomyocytes. The feasibility of remotely manipulating drug release and tissue properties was also demonstrated. This approach of combining functional electronics with biomaterials provided a new direction for exploration in cardiac tissue engineering.

### 3.5 Vascular tissue regeneration

Blood vessels are the conduits for blood circulation in the body, consisting of arteries, arterioles, capillaries, venules, and veins. Typically, arteries and veins are composed of three tissue layers, including a thick outermost layer (tunica adventitia or tunica externa) made of connective tissue, a thicker middle layer (tunica media) consisted of circularly arranged elastic fibers, connective tissue, and smooth muscle cells, and the thinnest inner layer (tunica intima) comprised of a single layer of endothelium supported by a subendothelial layer.<sup>192,193</sup> The delicate network of blood vessels provides cells with nutrients and oxygen for normal life activities while removing waste metabolic products.<sup>160,194</sup> Vascular diseases caused by damage to some major blood vessels such as coronary and carotid arteries are one of the leading causes of death.<sup>195,196</sup> Artificial blood vessel grafts can replace damaged blood vessels to ensure proper blood circulation. However, with the serious trend of cardiovascular diseases and the increasing aging of the population, the demand for artificial blood vessels has maintained a high growth rate. It remains a major medical task to develop artificial blood vessels with ideal properties. Based on the diameter and the applicable position in the body, artificial blood vessels are mainly divided into large-diameter (inner diameter > 6 mm) and small-diameter (inner diameter < 6 mm) artificial blood vessels. Among them, large-diameter artificial blood vessels have mature products widely used in the

clinic, while the preparation of small-diameter artificial blood vessels (SDBVs) is still an international challenge. This is due to the low patency rate of small-diameter artificial blood vessels, which may cause early thrombosis and poor endothelialization in the middle and late stages. Therefore, it is important to improve the proximal and distal patency rates of artificial blood vessels by rational design and modification.<sup>194</sup>

Electrospun fibers have significant advantages in the preparation of artificial blood vessels. The structure of electrospun fibers is similar to that of natural ECM, which can effectively enhance cell proliferation and adhesion, allowing for effective transport and exchange of substances. The surface roughness and modulus of the electrospun fibers can also be regulated to manipulate the material–cell interaction. In addition, the electrospun fiber network can be modified with bioactive functionalities to enhance cellular affinity, impart anticoagulant properties, and promote endothelialization.<sup>197</sup> Different types of cells can also be integrated into the multiple layers of one tube to mimic the multiple layer structure of a natural blood vessel. The mechanical properties of the artificial blood vessel based on electrospun fibers can be maintained and regulated to assure the mechanical stability and match with those of the native tissue. For artificial blood vessels, especially for SDBVs, thrombosis and other potentially fatal complications can be caused by even a slight mismatch in mechanical properties.<sup>2,198</sup> Therefore, the mechanical properties of artificial blood vessels are crucial to maintain the morphology and function of the material in the flowing blood. The mechanical properties of artificial blood vessels prepared by electrospinning can be more easily tuned than those from other processes, and nanofibers with target properties can be obtained by changing the raw materials or the parameters during or after electrospinning. The mechanical properties of electrospun nanofibers depend mainly on the molecular chain arrangement, crystallinity, macroscopic orientation, inter-fiber connection forms, and defects of the nanofibers. There are many ways to improve the mechanical properties of electrospun nanofibers, for example, the use of raw materials with excellent mechanical properties for electrospinning. In the study of artificial blood vessels, the use of elastomers is an effective method to improve their mechanical properties. In addition, appropriate filler materials can be added to improve the mechanical properties of the composite fibers. During the electrospinning process, the parameters can be varied to improve the orientation and the degree of crystallization in the nanofibers for enhancing the mechanical properties of the nanofibers. Moreover, a proper post-treatment of electrospun nanofibers can also improve their mechanical properties.

**3.5.1 Anticoagulation.** Thrombosis and resulting restenosis due to low patency within the vessels are the primary causes of failure in the regeneration of vascular tissue.<sup>199</sup> Therefore, an ideal electrospun fiber scaffold should have anticoagulant properties, which require good hemocompatibility of the implant.<sup>200,201</sup> The roughness of the graft surface is an important factor affecting hemocompatibility and behaviors of monolayer endothelial cells.<sup>202</sup> In one study, a bilayer vascular graft

was prepared, with an ultrathin smooth inner layer and a thick microfibrillar outer layer made of PCL by an ink printing method combined with electrospinning.<sup>203</sup> The nanofiber, microfiber, and bilayer vascular grafts were exposed to rabbit arterial blood flow for 1 h. Stereomicroscopy showed that the lumen of the bilayer grafts was unobstructed and clean without clotting, while the luminal surfaces of the nanofiber and microfiber grafts turned red (Fig. 7A). SEM images also demonstrated minimal platelet and plasma protein adhesion on the luminal surface of the bilayer grafts. This study suggested that such bilayer vascular grafts with a smooth inner layer exhibited excellent hemocompatibility without altering blood flow, which maintained patency within the graft and provided an attractive strategy for future applications in vascular tissue engineering.

Surface modification of electrospun fibers by loading bioactive substances can directly endow anticoagulation capability to the material. Heparin is a commonly used anticoagulant in clinical practice due to its significant role in reducing thrombus formation.<sup>204</sup> In addition, heparin can inhibit human vascular smooth muscle (HVSM) cell proliferation and prevent vascular occlusion.<sup>205</sup> The modification of grafted heparin on the inner surface of electrospun fibers results in anticoagulation. Zhang *et al.* doped bacterial nanocellulose in electrospun cellulose acetate microfibers and then immobilized heparin on the inner surface of the fibers.<sup>206</sup> It was found that platelet adhesion was significantly reduced, and antithrombotic behavior was greatly enhanced on the vascular grafts loaded with heparin compared with other two groups of electrospun cellulose acetate microfibers

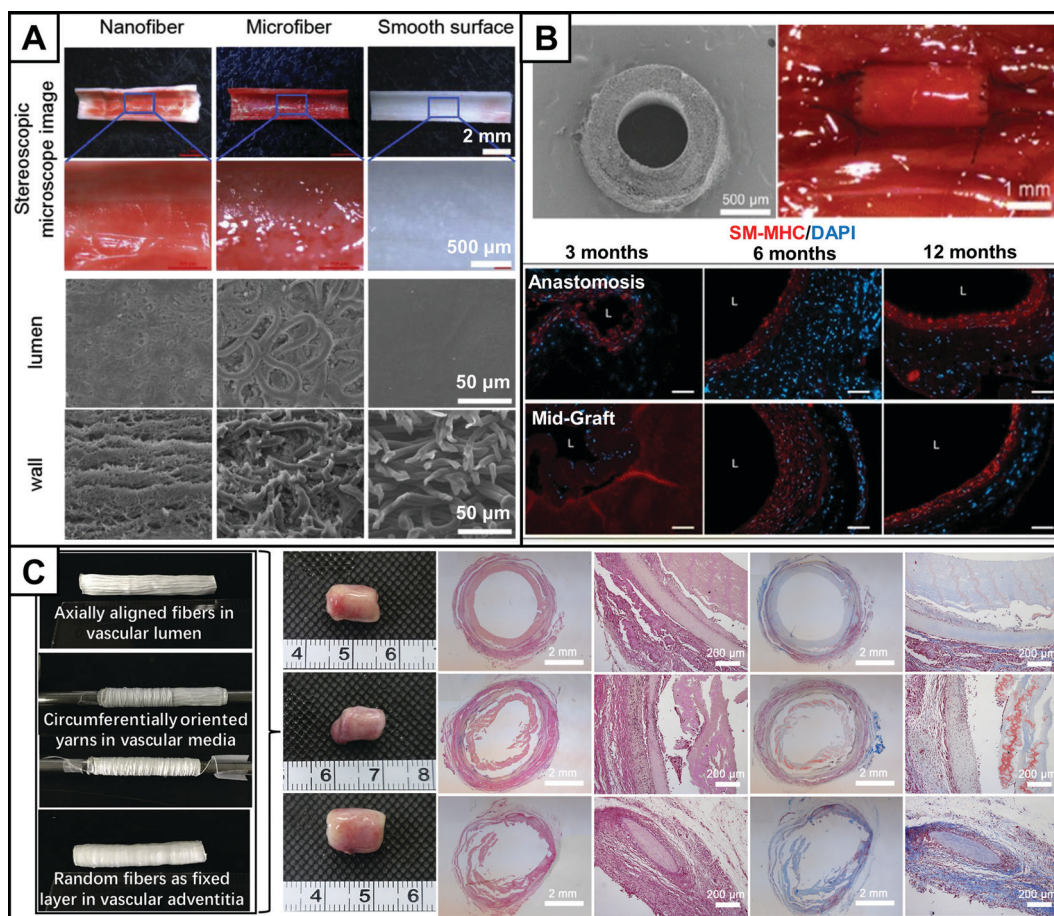


**Fig. 7** Electrospun nanofiber scaffolds in vascular tissue engineering. (A) Stereoscopic images of the lumen of three grafts exposed to an artery for 1 h using a rabbit arteriovenous shunt (AV-shunt), showing the absence of coagulation generation in the bilayer vascular grafts (above). SEM images of the lumen and cross-section showing minimal platelets and plasma proteins on the lumen and inner surface of the bilayer grafts compared to the other two groups, demonstrating the ability of this bilayer vascular graft to resist coagulation (below). (B) SEM image of electrospun nanofiber vascular grafts with a bilayer tubular structure (upper left). A picture of the site where the graft was implanted into the vessel (upper right). Immunohistochemical staining for markers of late differentiation of smooth muscle (SM-MHC) (red) and DAPI (blue) at 3, 6 and 12 months, with a ring-like distribution of red and blue fluorescence at 6 months, demonstrating differentiation of inner smooth muscle cells in the inner layer (below) (40 $\times$  magnification). (C) Schematic diagram of the structure of the three layers of the tubular graft (left). The grafts were examined morphologically at 2, 6, and 10 weeks after subcutaneous grafting, and the tubular structure was well maintained (middle). H&E staining and Masson trichrome staining were used for histological analysis of the cross-sections of the grafts after 2, 6 and 10 weeks of subcutaneous transplantation. It was observed by H&E staining that the grafts were gradually wrapped by regenerated tissue while maintaining a certain graft structure, and Masson trichrome staining demonstrated the regeneration of collagen, providing a bionic microenvironment to promote tissue regeneration (right). (A–C) Reprinted with permission from ref. 203: Copyright (2018) Elsevier, ref. 212: Copyright (2016) Springer Nature, and ref. 217: Copyright (2018) Elsevier, respectively.

and cellulose acetate microfibers doped with bacterial nanocellulose. The heparin showed a sudden release at the initial stage of implantation, resulting in lower levels of heparin release at later stages, which can be further improved. A sustained release of heparin will be ideal to achieve the long-term anticoagulation goal. For instance, a PCL electrospun nanofiber scaffold was modified using a nanocoating encapsulated with gelatin, polylysine, and heparin by a self-assembly technique.<sup>207</sup> Under physiological conditions, the nanocoating could responsively release a variety of bioactive molecules, significantly reducing platelet adhesion. Most importantly, this scaffold achieved the controlled release of heparin and extended the release duration to 35 days, allowing for sustained delivery of anticoagulants to the body.

**3.5.2 Re-endothelialization.** Prevention of coagulation and inhibition of thrombosis are prerequisites for endothelial formation.<sup>208</sup> Impaired function of endothelial cells can lead to endothelial cell hyperplasia, ultimately resulting in the narrow embolization and ineffectiveness of the graft.<sup>209</sup> Complete endothelialization can fundamentally address the problems of thrombosis and endothelial hyperplasia. The key to re-endothelialization is the adhesion, proliferation, and directional differentiation of endothelial cells.<sup>210,211</sup> Therefore, how to achieve rapid re-endothelialization is a crucial factor to consider for constructing artificial vascular grafts. In one study, a bilayer electrospun nanofiber vascular graft was fabricated, with an inner layer of polyglycerol sebacate and an outer layer of PCL to provide mechanical support.<sup>212</sup> It was implanted to remodel arteries in a mouse model (Fig. 7B). Immunofluorescence staining showed that at 6 months after implantation, differentiation of smooth muscle cells appeared in the inner layer of the scaffold, which continued until 12 months, promoting re-endothelialization of the vessel. Meanwhile, the scaffold further enhanced remodeling of the aorta adjacent to the damaged site, and there was no thrombosis at 12 months. This grafting strategy was expected to improve the long-term efficacy of the graft.

Selective binding of endothelialization-promoting factors enables electrospun fibers to have excellent bioactivity and contribute to vascular regeneration. For example, the loading of VEGF enables the inner layer of artificial blood vessels to promote increased vascular permeability, accelerate vascular endothelial cell migration, and regulate proliferation and angiogenesis. By loading PDGF, the inner surface of the artificial blood vessels can not only accelerate the formation of neovascularization but also recruit endothelial cells and promote the proliferation and migration of the cells.<sup>213</sup> In one study, VEGF was loaded into the core layer of PLGA nanofibers by coaxial electrospinning.<sup>214</sup> Along with the degradation of the materials, VEGF could diffuse out and was continuously released for more than 28 days, promoting the proliferation of endothelial cells. In another study, VEGF<sub>165</sub> and heparin were co-encapsulated in the core layer of poly(L-lactide-co-caprolactone)[P(LLA-CL)]-collagen/elastin electrospun core-sheath fibers.<sup>215</sup> The graft enabled the sustained release of heparin and VEGF<sub>165</sub>, maintaining the local concentrations of

the factors over a typical period of time at the target site. It significantly promoted the adhesion and proliferation of human aortic endothelial cells *in vitro*, and no coagulation was observed *in vivo* while the formation of endothelialization was promoted. In addition, Jin *et al.* utilized the good mechanical properties of poly(L-propylene-co-ε-caprolactone) (PLCL) and the hydrophilicity of the filamentous protein (SF) to fabricate an electrospun bilayer nanofiber vascular scaffold equipped with heparin.<sup>216</sup> This PLCL/SF/Hep implantation in rabbit neck showed no coagulation within 3 months, while a continuous new intimal layer formed spontaneously. These studies have demonstrated the importance of the sustained release of growth factors to maintain the long-term effects of artificial blood vessels.

Given that natural blood vessels have a three-layer structure, artificial blood vessels with a three-layer structure can be obtained by regulating the material composition, diameters, and pore sizes of the fibers deposited at different stages. This three-layer structure can better mimic the structure and composition of natural blood vessels and exert bionic properties, thus accelerating the construction of neovascularization. For example, a three-layer artificial blood vessel was designed by a three-step electrospinning method, including uniaxially aligned PLCL/collagen (COL) fibers, circumferentially arranged PLGA/SF yarns, and random PLCL/COL fibers, respectively, from the inside out (Fig. 7C).<sup>217</sup> The innermost layer was able to promote endothelial cell adhesion, the middle layer could regulate the morphology and proliferation of smooth muscle cells (SMCs), and the outermost layer provided mechanical support for the scaffold. The tubular structure of the graft essentially remained unchanged after 2, 6, and 10 weeks of implantation. H&E and Masson staining showed that the implanted triple-layered tubular grafts had good cellular infiltration ability and could promote vascular tissue regeneration. Given their bionic structural properties, the electrospun triple-layer nanofiber scaffolds show great potential in clinical trials and are expected to advance the clinical translation of artificial blood vessels.

Currently, electrospinning has been widely applied in vascular tissue engineering. The adjustable mechanical properties of electrospun fibers can provide suitable mechanical performance for the flow of blood. The anticoagulation and re-endothelialization can be further achieved by designing fiber scaffolds with different structures and functions. In the future, researchers need to conduct comprehensive design and performance comparisons from multiple perspectives, such as material types, molecular structures, molding technologies, bionic design, and bio-coating, to develop small-diameter artificial blood vessels with excellent biocompatibility and anticoagulation properties, contributing to solve major medical challenges and bring hope for the cure for patients with cardiovascular diseases.

### 3.6 Ocular tissue regeneration

The eye is a small and delicate organ in the human body responsible for vision.<sup>218</sup> Since most of its cells are terminally differentiated, damage to these cells can easily lead to loss of

vision or even blindness.<sup>219</sup> Currently, clinical transplantation therapy for ocular diseases is faced with risks such as donor shortage and immune rejection. Therefore, it is of clinical significance to develop bioactive materials that can promote ocular tissue regeneration.<sup>218,220</sup> Electrospun fibers can promote cell adhesion and proliferation, greatly improving the survival rate of transplanted cells. In addition, electrospun fibers can be easily modified, and functionalized fibrous scaffolds have great potential for ocular tissue engineering applications.

**3.6.1 Survival of monolayer cells.** Among ocular tissues, retinal pigment epithelium (RPE) is a critical part of the eye used for light perception, and defects in RPE can lead to vision problems.<sup>221</sup> As a common cause of blindness, RPE degeneration can lead to degenerative retinal diseases, such as RPE dysfunction, age-related macular degeneration, and Stargard's disease. No effective drugs or methods have been developed clinically to treat RPE degeneration.<sup>222,223</sup> RPE cell transplantation is currently the only promising treatment for RPE dysfunction. However, it is not sufficient to reconstruct the complex cellular architecture of the RPE, and the delivery and survival of RPE cells are also a great challenge.<sup>224</sup> From previous studies, it is known that, when RPE cells are injected directly, the cells may reflux into the vitreous cavity, thus blocking the optical pathway and even causing retinal detachment.<sup>225</sup> More seriously, a rapid injection of RPE cells may lead to massive cell death.<sup>226</sup>

Although there are no studies of electrospun fibers as scaffolds for RPE cell transplantation, there are examples of other types of polymeric membranes for ocular tissue regeneration. Currently, the main research in RPE cell transplantation is focused on carrying monolayers of cells or cell suspensions on polymer membranes.<sup>227</sup> For example, an ultrathin film composed of poly(parylene) was prepared and used as the support for a monolayer of cells.<sup>228</sup> It was found that on the membrane, the survival rate of monolayer RPE cells was improved compared to the cell suspension. Reflux was observed on the sclera after the cell suspension was injected, which explained the low survival rate of RPE cells by this method. In addition, the implantation of a monolayer of RPE cells could prevent the cell folding, which was beneficial for a faster recovery and the maintenance of the epithelial phenotype, demonstrating that the monolayer morphology of RPE cells may play an important role in the repair of the rat retina. Yaji *et al.* fabricated a RPE cell sheet using the poly(*N*-isopropylacrylamide) (PIPAAm) membrane, and the post-transplantation results showed that the monolayer structure of the RPE cell sheet could adhere more effectively under the neuroretina for repair than a direct injection of the isolated cell suspension.<sup>229</sup>

These existing studies also give guidance on the use of electrospun fibers for RPE cell transplantation. The most critical factor in RPE transplantation is the adhesion and survival of monolayer cells. Electrospun fibers have been extensively investigated for *in vivo* cell delivery due to their good biocompatibility and ability to promote cell adhesion. Active substances such as drugs or proteins can be easily loaded into electrospun fibers, which not only promote the adhesion and

proliferation of exogenous cells, but also improve the ocular microenvironment and contribute to the repair and regeneration of endogenous cells. Therefore, the great potential of electrospun fibers in RPE cell transplantation and inhibition of RPE degeneration can be anticipated.

In addition to RPE cell transplantation, stem cell transplantation can also be applied to treat degenerative retinal diseases. The U.S. Food and Drug Administration has approved several cell types for use in clinical trials for the treatment of degenerative retinal diseases. Current promising stem cells for the treatment of degenerative retinal diseases include retinal precursor cells (RPCs), MSCs, ESCs, and iPSCs. RPCs can develop into various types of retinal cells that contribute to the maintenance of visual function after photoreceptor cell injury. MSCs, ESCs, and iPSCs are required for directed differentiation into RPE cells for further treatment of degenerative retinal diseases. *In situ* delivery of stem cells using electrospun nanofiber scaffolds as carriers is an effective strategy for stem cell transplantation. There have been numerous studies on electrospun nanofibers for exogenous stem cell delivery in many tissue injury repairs. In addition to the controlled delivery of stem cells, electrospun nanofiber scaffolds can also regulate their migration and differentiation, which greatly improves the therapeutic efficiency of stem cells. For the treatment of degenerative retinal diseases, by designing the composition and structure of electrospun nanofiber scaffolds and introducing bioactive substances into the scaffolds, the migration of stem cells to the photoreceptor sites can be promoted, and their directed differentiation into PRE cells can be regulated, which is expected to realize the regeneration of ocular tissues and enable patients to regain their sight.

**3.6.2 Corneal epithelial cell growth and proliferation.** Corneal epithelial cells and corneal limbal epithelial cells (LECs) are also important functional cells in the eye tissue that determine the vision.<sup>230</sup> LECs can positively affect corneal healing by reducing local inflammation.<sup>231</sup> Corneal limbal stem cell deficiency (LSCD) can be triggered in cases of chemical damage, radiation and burns to the cornea, as well as contact lens-induced keratopathy and ocular surface failure.<sup>232</sup> LSCD prevents the differentiation of corneal limbal stem cells to corneal epithelial cells and LECs, thus affecting visual acuity.<sup>233</sup> Corneal rim transplantation is currently the main method for the treatment of ocular diseases such as LSCD, which involves the transplantation of cultured corneal rim cells onto human amniotic membrane for implantation into the eye.<sup>220</sup> However, the disadvantages of amniotic membrane, such as weakness in mechanical properties, difficulty in material handling, and susceptibility to transmit viral diseases, limit its application in ocular tissue engineering.<sup>221</sup>

Taking advantage of the excellent mechanical properties and cytocompatibility of electrospun fibers, they can be applied for the culture and transplantation of corneal cells, avoiding the shortcomings of the amniotic membrane. Studies have shown that electrospun fibers can promote the growth and proliferation of LECs. In one study, an electrospun poly(3-hydroxybutyrate-co-3-hydroxyvalerate) nanofiber membrane was fabricated and applied

as an alternative to the amniotic membrane to support corneal limbal stem cells.<sup>234</sup> The nanofibrous membrane was highly biocompatible and could provide an environment for the growth and proliferation of stem cells, suggesting the possibility of manufacturing a novel biomaterial with good biocompatibility and mechanical properties as the scaffold for ocular tissue engineering.

In addition, electrospun fibers can be modified to regulate their properties for suiting the application requirements.<sup>235</sup> After treating an electrospun PCL nanofiber scaffold with plasma (He/O), its wettability and transparency were both improved in comparison with those of the pure PCL scaffold, which could effectively promote the growth, adhesion, and proliferation of LECs.<sup>236</sup> Although electrospun nanofibers have not yet been widely used for ocular tissue engineering studies, their unique advantages cannot be ignored. In the future, with good utilization, electrospun nanofiber scaffolds with capabilities of excellent mechanical properties, biocompatibility, promotion of cell adhesion and proliferation, and controlled drug delivery can contribute to the development of ocular tissue engineering.

## 4. Conclusions and perspectives

Electrospun nanofibers are of great importance for soft tissue regeneration. By regulating the parameters of electrospinning and the collection process, it is possible to obtain nanofibers with various structures. The diameter, orientation, porosity, and surface morphology of the nanofibers have an influence on cell behaviors. Electrospun fibers mimic the ECM to establish contact and signal communication with cells, thus manipulating cell proliferation, migration, differentiation, and other behaviors. By modulating cellular behaviors, electrospun nanofibers can further promote tissue regeneration. Electrospun fibrous scaffolds are prepared to meet the regenerative needs of different tissues according to their characteristics. By modulating the surface morphology or gradient structure of electrospun fibers, they can provide topographical cues and tropism for tissue regeneration. By loading or depositing bioactive substances or cells into/onto electrospun fibers, they can provide biochemical cues for tissue regeneration. Combining topographic design, controlled delivery of bioactive substances, and cellular composition, electrospun fibrous scaffolds have promoted the repair of various soft tissues such as nerves (peripheral nerves and central nerves), skin, heart, blood vessels, and cornea. Electrospun fibers have been extensively studied in the field of tissue regeneration, and how to effectively integrate multiple guidance signals based on existing studies is still a key issue to be addressed in the future. In addition to the focus on the material itself, imaging monitoring of the treatment process and external stimulation interventions are also of great significance for regeneration and rehabilitation. After surgery, a real-time monitoring of the rehabilitation process guided by imaging technologies, along with the introduction of external stimuli to activate the functional recovery of damaged tissues at specific stages, is crucial for the complete tissue

repair process. Therefore, a comprehensive platform for treatment, monitoring, assessment, and rehabilitation, will be promising and responsive to the actual needs to achieve translation from research to clinic, from laboratory to market, and to effectively address the major issues of human life and health.

## Conflicts of interest

The authors declare no competing financial interest.

## Acknowledgements

This work is supported by the National Natural Science Foundation of China (Grant No. 52073014 and 82002049; to J. X.), Key Program of Beijing Natural Science Foundation (Z200025), and Fundamental Research Funds for the Central Universities (buctrc202020). This work was also supported by the opening Foundation of State Key Laboratory of Organic-Inorganic Composites, Beijing University of Chemical Technology (oic-202201004).

## References

- 1 W. A. Palispis and R. Gupta, *Exp. Neurol.*, 2017, **290**, 106–114.
- 2 D. Wang, Y. Xu, Q. Li and L. S. Turng, *J. Mater. Chem. B*, 2020, **8**, 1801–1822.
- 3 A. K. Capulli, L. A. MacQueen, S. P. Sheehy and K. K. Parker, *Adv. Drug Delivery Rev.*, 2016, **96**, 83–102.
- 4 Y. Ikada, *J. R. Soc., Interface*, 2006, **3**, 589–601.
- 5 M. Doostmohammadi, H. Forootanfar and S. Ramakrishna, *Mater. Sci. Eng., C*, 2020, **109**, 110521.
- 6 K. W. Lee, D. B. Stolz and Y. Wang, *Proc. Natl. Acad. Sci. U. S. A.*, 2011, **108**, 2705–2710.
- 7 W. P. Daley, S. B. Peters and M. Larsen, *J. Cell Sci.*, 2008, **121**, 255–264.
- 8 J. G. Jacot, A. D. McCulloch and J. H. Omens, *Biophys. J.*, 2008, **95**, 3479–3487.
- 9 G. Michel, T. Tonon, D. Scornet, J. M. Cock and B. Kloareg, *New Phytol.*, 2010, **188**, 82–97.
- 10 F. Rosso, A. Giordano, M. Barbarisi and A. Barbarisi, *J. Cell. Physiol.*, 2004, **199**, 174–180.
- 11 J. Xue, T. Wu, Y. Dai and Y. Xia, *Chem. Rev.*, 2019, **119**, 5298–5415.
- 12 X. Wan, Y. Zhao, Z. Li and L. Li, *Exploration*, 2022, **2**, 20210029.
- 13 J. Xue, J. Xie, W. Liu and Y. Xia, *Acc. Chem. Res.*, 2017, **50**, 1976–1987.
- 14 S. Agarwal, J. H. Wendorff and A. Greiner, *Adv. Mater.*, 2009, **21**, 3343–3351.
- 15 L. Zhan, J. Deng, Q. Ke, X. Li, Y. Ouyang, C. Huang, X. Liu and Y. Qian, *Adv. Fiber Mater.*, 2021, 1–11, DOI: [10.1007/s42765-021-00116-5](https://doi.org/10.1007/s42765-021-00116-5).
- 16 T. Wu, J. Xue, H. Li, C. Zhu, X. Mo and Y. Xia, *ACS Appl. Mater. Interfaces*, 2018, **10**, 8536–8545.

- 17 J. Xue, M. He, H. Liu, Y. Niu, A. Crawford, P. D. Coates, D. Chen, R. Shi and L. Zhang, *Biomaterials*, 2014, **35**, 9395–9405.
- 18 J. Xue, C. Zhu, J. Li, H. Li and Y. Xia, *Adv. Funct. Mater.*, 2018, **28**, 1705563.
- 19 X. Gao, S. Han, R. Zhang, G. Liu and J. Wu, *J. Mater. Chem. B*, 2019, **7**, 7075–7089.
- 20 M. C. Bonferoni, C. Caramella, L. Catenacci, B. Conti, R. Dorati, F. Ferrari, I. Genta, T. Modena, S. Perteghella, S. Rossi, G. Sandri, M. Sorrenti, M. L. Torre and G. Tripodo, *Pharmaceutics*, 2021, **13**, 1341.
- 21 J. Pelipenko, P. Kocbek and J. Kristl, *Int. J. Pharm.*, 2015, **484**, 57–74.
- 22 D. Li and Y. Xia, *Adv. Mater.*, 2004, **16**, 1151–1170.
- 23 G. Yang, X. L. Li, Y. He, J. K. Ma, G. L. Ni and S. B. Zhou, *Prog. Polym. Sci.*, 2018, **81**, 80–113.
- 24 H. Wu, J. Fan, C. C. Chu and J. Wu, *J. Mater. Sci.: Mater. Med.*, 2010, **21**, 3207–3215.
- 25 G. Yan, J. Yu, Y. Qiu, X. Yi, J. Lu, X. Zhou and X. Bai, *Langmuir*, 2011, **27**, 4285–4289.
- 26 S. Eom, S. M. Park, H. Hong, J. Kwon, S. R. Oh, J. Kim and D. S. Kim, *ACS Appl. Mater. Interfaces*, 2020, **12**, 51212–51224.
- 27 A. Luraghi, F. Peri and L. Moroni, *J. Controlled Release*, 2021, **334**, 463–484.
- 28 M. Rahmati, D. K. Mills, A. M. Urbanska, M. R. Saeb, J. R. Venugopal, S. Ramakrishna and M. Mozafari, *Prog. Mater. Sci.*, 2021, **117**, 100721.
- 29 J. Xue, T. Wu and Y. Xia, *APL Mater.*, 2018, **6**, 120902.
- 30 P.-Y. Chen and S.-H. Tung, *Macromolecules*, 2017, **50**, 2528–2534.
- 31 J. Wang, H. B. Yao, D. He, C. L. Zhang and S. H. Yu, *ACS Appl. Mater. Interfaces*, 2012, **4**, 1963–1971.
- 32 Y. Zhao, X. Cao and L. Jiang, *J. Am. Chem. Soc.*, 2007, **129**, 764–765.
- 33 M. A. Schwartz and A. R. Horwitz, *Cell*, 2006, **125**, 1223–1225.
- 34 E. H. Barriga and R. Mayor, *Curr. Top. Dev. Biol.*, 2015, **112**, 301–323.
- 35 C. H. Feng, Y. C. Cheng and P. H. Chao, *Acta Biomater.*, 2013, **9**, 5502–5510.
- 36 K. M. Stroka, H. Jiang, S. H. Chen, Z. Tong, D. Wirtz, S. X. Sun and K. Konstantopoulos, *Cell*, 2014, **157**, 611–623.
- 37 H. Y. Mi, M. R. Salick, X. Jing, W. C. Crone, X. F. Peng and L. S. Turng, *J. Biomed. Mater. Res. A*, 2015, **103**, 593–603.
- 38 J. Xue, T. Wu, J. Qiu, S. Rutledge, M. L. Tanes and Y. Xia, *Adv. Funct. Mater.*, 2020, **30**, 2002031.
- 39 J. Xue, T. Wu, J. Qiu and Y. Xia, *Small Methods*, 2020, **4**, 2000125.
- 40 J. Xie, M. R. Macewan, W. Z. Ray, W. Liu, D. Y. Siewe and Y. Xia, *ACS Nano*, 2010, **4**, 5027–5036.
- 41 J. Xue, T. Wu, J. Qiu and Y. Xia, *Part. Part. Syst. Character.*, 2022, **39**, 2100280.
- 42 N. F. Huang, S. Patel, R. G. Thakar, J. Wu, B. S. Hsiao, B. Chu, R. J. Lee and S. Li, *Nano Lett.*, 2006, **6**, 537–542.
- 43 B. Jankovic, J. Pelipenko, M. Skarabot, I. Musevic and J. Kristl, *Int. J. Pharm.*, 2013, **455**, 338–347.
- 44 J. Xie, X. Li, J. Lipner, C. N. Manning, A. G. Schwartz, S. Thomopoulos and Y. Xia, *Nanoscale*, 2010, **2**, 923–926.
- 45 J. Xie, M. R. MacEwan, W. Liu, N. Jesuraj, X. Li, D. Hunter and Y. Xia, *ACS Appl. Mater. Interfaces*, 2014, **6**, 9472–9480.
- 46 T. Reya, S. J. Morrison, M. F. Clarke and I. L. Weissman, *Nature*, 2001, **414**, 105–111.
- 47 W. Chen, Y. Shao, X. Li, G. Zhao and J. Fu, *Nano Today*, 2014, **9**, 759–784.
- 48 M. J. Dalby, N. Gadegaard and R. O. Oreffo, *Nat. Mater.*, 2014, **13**, 558–569.
- 49 M. B. Taskin, R. Xu, H. Gregersen, J. V. Nygaard, F. Besenbacher and M. Chen, *ACS Appl. Mater. Interfaces*, 2016, **8**, 15864–15873.
- 50 G. T. Christopherson, H. Song and H. Q. Mao, *Biomaterials*, 2009, **30**, 556–564.
- 51 A. Portone, M. Moffa, C. Gardin, L. Ferroni, M. Tatullo, F. Fabbri, L. Persano, A. Piattelli, B. Zavan and D. Pisignano, *Adv. Funct. Mater.*, 2019, **29**, 1806694.
- 52 M. N. Andalib, J. S. Lee, L. Ha, Y. Dzenis and J. Y. Lim, *Biochem. Biophys. Res. Commun.*, 2016, **473**, 920–925.
- 53 C. Li, C. Vepari, H. J. Jin, H. J. Kim and D. L. Kaplan, *Biomaterials*, 2006, **27**, 3115–3124.
- 54 N. Zhang, Q.-R. Xiao, X.-Y. Man, H.-X. Liu, L.-X. Lü and N.-P. Huang, *RSC Adv.*, 2016, **6**, 22144–22152.
- 55 L. Xia, K. Lin, X. Jiang, B. Fang, Y. Xu, J. Liu, D. Zeng, M. Zhang, X. Zhang, J. Chang and Z. Zhang, *Biomaterials*, 2014, **35**, 8514–8527.
- 56 X. Jiang, H. Q. Cao, L. Y. Shi, S. Y. Ng, L. W. Stanton and S. Y. Chew, *Acta Biomater.*, 2012, **8**, 1290–1302.
- 57 Z. Bagher, M. Azami, S. Ebrahimi-Barough, H. Mirzadeh, A. Solouk, M. Soleimani, J. Ai, M. R. Nourani and M. T. Joghataei, *Mol. Neurobiol.*, 2016, **53**, 2397–2408.
- 58 Y. C. Jiang, X. F. Wang, Y. Y. Xu, Y. H. Qiao, X. Guo, D. F. Wang, Q. Li and L. S. Turng, *Biomacromolecules*, 2018, **19**, 3747–3753.
- 59 L. Mohammadi Amirabad, M. Massumi, M. Shamsara, I. Shabani, A. Amari, M. Mossahebi Mohammadi, S. Hosseinzadeh, S. Vakilian, S. K. Steinbach, M. R. Khorramzadeh, M. Soleimani and J. Barzin, *ACS Appl. Mater. Interfaces*, 2017, **9**, 6849–6864.
- 60 S. M. Damaraju, Y. Shen, E. Elele, B. Khusid, A. Eshghinejad, J. Li, M. Jaffe and T. L. Arinze, *Biomaterials*, 2017, **149**, 51–62.
- 61 J. Scheib and A. Hoke, *Nat. Rev. Neurol.*, 2013, **9**, 668–676.
- 62 Y. Qian, H. Lin, Z. Yan, J. Shi and C. Fan, *Mater. Today*, 2021, **51**, 165–187.
- 63 A. L. Cattin, J. J. Burden, L. Van Emmenis, F. E. Mackenzie, J. J. Hoving, N. Garcia Calavia, Y. Guo, M. McLaughlin, L. H. Rosenberg, V. Quereda, D. Jamecna, I. Napoli, S. Parrinello, T. Enver, C. Ruhrberg and A. C. Lloyd, *Cell*, 2015, **162**, 1127–1139.
- 64 P. Meena, A. Kakkar, M. Kumar, N. Khatri, R. K. Nagar, A. Singh, P. Malhotra, M. Shukla, S. K. Saraswat, S. Srivastava, R. Datt and S. Pandey, *Cell Tissue Res.*, 2020, **383**, 617–644.



- 65 M. D. Sarker, S. Naghieh, A. D. McInnes, D. J. Schreyer and X. Chen, *Prog. Neurobiol.*, 2018, **171**, 125–150.
- 66 C. R. Carvalho, J. Silva-Correia, J. M. Oliveira and R. L. Reis, *Adv. Drug Delivery Rev.*, 2019, **148**, 308–343.
- 67 X. Gu, F. Ding and D. F. Williams, *Biomaterials*, 2014, **35**, 6143–6156.
- 68 Z. Wang, Y. Cui, J. Wang, X. Yang, Y. Wu, K. Wang, X. Gao, D. Li, Y. Li, X. L. Zheng, Y. Zhu, D. Kong and Q. Zhao, *Biomaterials*, 2014, **35**, 5700–5710.
- 69 Y. Jia, W. Yang, K. Zhang, S. Qiu, J. Xu, C. Wang and Y. Chai, *Acta Biomater.*, 2019, **83**, 291–301.
- 70 X. Dong, S. Liu, Y. Yang, S. Gao, W. Li, J. Cao, Y. Wan, Z. Huang, G. Fan, Q. Chen, H. Wang, M. Zhu and D. Kong, *Biomaterials*, 2021, **272**, 120767.
- 71 J. R. Potas, F. Haque, F. L. Maclean and D. R. Nisbet, *J. Immunol. Methods*, 2015, **420**, 38–49.
- 72 X. Chen, X. M. Ge, Y. Qian, H. Z. Tang, J. L. Song, X. H. Qu, B. Yue and W. E. Yuan, *Adv. Funct. Mater.*, 2020, **30**, 2004537.
- 73 D. Lv, L. Zhou, X. Zheng and Y. Hu, *Eur. J. Neurosci.*, 2017, **45**, 1258–1267.
- 74 C. Simitzi, A. Ranella and E. Stratakis, *Acta Biomater.*, 2017, **51**, 21–52.
- 75 T. Wu, J. Xue and Y. Xia, *Angew. Chem., Int. Ed.*, 2020, **59**, 15626–15632.
- 76 J. Xue, T. Wu, J. Li, C. Zhu and Y. Xia, *Angew. Chem., Int. Ed.*, 2019, **58**, 3948–3951.
- 77 J. Xue, H. Li and Y. Xia, *Macromol. Biosci.*, 2018, **18**, e1800090.
- 78 J. Wang, H. Xiong, T. Zhu, Y. Liu, H. Pan, C. Fan, X. Zhao and W. W. Lu, *ACS Nano*, 2020, **14**, 12579–12595.
- 79 B. V. Lien, N. J. Brown, S. C. Ransom, B. M. Lechrich, S. Shahrestani, A. R. Tafreshi, R. C. Ransom and R. Sahyouni, *J. Peripher. Nerv. Syst.*, 2020, **25**, 320–334.
- 80 M. Antman-Passig, J. Giron, M. Karni, M. Motiei, H. Schori and O. Shefi, *Adv. Funct. Mater.*, 2021, **31**, 2010837.
- 81 W. Chang, M. B. Shah, G. Zhou, K. Walsh, S. Rudraiah, S. G. Kumbar and X. Yu, *Biomed. Mater.*, 2020, **15**, 035003.
- 82 S. Chen, Z. Du, J. Zou, S. Qiu, Z. Rao, S. Liu, X. Sun, Y. Xu, Q. Zhu and X. Liu, *ACS Appl. Mater. Interfaces*, 2019, **11**, 17167–17176.
- 83 L. Zhu, S. J. Jia, T. J. Liu, L. Yan, D. G. Huang, Z. Y. Wang, S. Chen, Z. P. Zhang, W. Zeng, Y. Zhang, H. Yang and D. J. Hao, *Adv. Funct. Mater.*, 2020, **30**, 2002610.
- 84 Y. X. Wu, H. Ma, J. L. Wang and W. Qu, *Neural Regener. Res.*, 2021, **16**, 1093–1098.
- 85 J. Xue, J. Yang, D. M. O'Connor, C. Zhu, D. Huo, N. M. Boullis and Y. Xia, *ACS Appl. Mater. Interfaces*, 2017, **9**, 12299–12310.
- 86 G. Li, T. Zheng, L. Wu, Q. Han, Y. Lei, L. Xue, L. Zhang, X. Gu and Y. Yang, *Sci. Adv.*, 2021, **7**, eabi5812.
- 87 S. Ghosh, S. Haldar, S. Gupta, A. Bisht, S. Chauhan, V. Kumar, P. Roy and D. Lahiri, *ACS Appl. Bio. Mater.*, 2020, **3**, 5796–5812.
- 88 J. Wang, Y. Cheng, L. Chen, T. Zhu, K. Ye, C. Jia, H. Wang, M. Zhu, C. Fan and X. Mo, *Acta Biomater.*, 2019, **84**, 98–113.
- 89 L. Wang, C. Lu, S. Yang, P. Sun, Y. Wang, Y. Guan, S. Liu, D. Cheng, H. Meng, Q. Wang, J. He, H. Hou, H. Li, W. Lu, Y. Zhao, J. Wang, Y. Zhu, Y. Li, D. Luo, T. Li, H. Chen, S. Wang, X. Sheng, W. Xiong, X. Wang, J. Peng and L. Yin, *Sci. Adv.*, 2020, **6**, eabc6686.
- 90 B. Gong, X. Zhang, A. Zahrani, W. Gao, G. Ma, L. Zhang and J. Xue, *Exploration*, 2022, **2**, 20210035.
- 91 R. M. Ransohoff and B. Engelhardt, *Nat. Rev. Immunol.*, 2012, **12**, 623–635.
- 92 T. Taoka, A. Fukusumi, T. Miyasaka, H. Kawai, T. Nakane, K. Kichikawa and S. Naganawa, *Radiographics*, 2017, **37**, 281–297.
- 93 B. A. Kakulas, *J. Spinal Cord Med.*, 1999, **22**, 119–124.
- 94 S. Ahmed, H. Venigalla, H. M. Mekala, S. Dar, M. Hassan and S. Ayub, *Indian J. Psychol. Med.*, 2017, **39**, 114–121.
- 95 E. Llorens-Bobadilla, J. M. Chell, P. Le Merre, Y. Wu, M. Zamboni, J. Bergenstrahle, M. Stenudd, E. Sopova, J. Lundeberg, O. Shupliakov, M. Carlen and J. Frisen, *Science*, 2020, **370**, eabb8795.
- 96 P. F. Stahel, T. VanderHeiden and M. A. Finn, *Curr. Opin. Crit. Care*, 2012, **18**, 651–660.
- 97 N. P. Visavadiya, S. P. Patel, J. L. VanRooyen, P. G. Sullivan and A. G. Rabchevsky, *Redox. Biol.*, 2016, **8**, 59–67.
- 98 A. Zendedel, F. Monnink, G. Hassanzadeh, A. Zaminy, M. M. Ansar, P. Habib, A. Slowik, M. Kipp and C. Beyer, *Mol. Neurobiol.*, 2018, **55**, 1364–1375.
- 99 A. R. D'Amato, D. L. Puhl, S. A.-T. Ellman, B. Balouch, R. J. Gilbert and E. F. Palermo, *Nat. Commun.*, 2019, **10**, 4830.
- 100 H. Algattas and J. H. Huang, *Int. J. Mol. Sci.*, 2013, **15**, 309–341.
- 101 A. K. Shetty, V. Mishra, M. Kodali and B. Hattiangady, *Front. Cell. Neurosci.*, 2014, **8**, 404.
- 102 F. L. Maclean, C. L. Lau, S. Ozergun, R. D. O'Shea, C. Cederfur, J. Wang, K. E. Healy, F. R. Walker, D. Tomas, M. K. Horne, P. M. Beart and D. R. Nisbet, *J. Mater. Chem. B*, 2017, **5**, 4073–4083.
- 103 S. Lee, S. Yun, K. I. Park and J. H. Jang, *ACS Nano*, 2016, **10**, 3282–3294.
- 104 Z. Peng, X. Li, M. Fu, K. Zhu, L. Long, X. Zhao, Q. Chen, D. Y.-B. Deng and Y. Wan, *J. Neurochem.*, 2019, **150**, 709–722.
- 105 L. H. Nguyen, M. Gao, J. Lin, W. Wu, J. Wang and S. Y. Chew, *Sci. Rep.*, 2017, **7**, 42212.
- 106 X. Sun, C. Zhang, J. Xu, H. Zhai, S. Liu, Y. Xu, Y. Hu, H. Long, Y. Bai and D. Quan, *ACS Biomater. Sci. Eng.*, 2020, **6**, 1228–1238.
- 107 N. K. Mohtaram, J. Ko, A. Agbay, D. Rattray, P. O. Neill, A. Rajwani, R. Vasandani, H. L. Thu, M. B.-G. Jun and S. M. Willerth, *J. Mater. Chem. B*, 2015, **3**, 7974–7985.
- 108 S. Smith, K. Goodge, M. Delaney, A. Struzyk, N. Tansey and M. Frey, *Nanomaterials*, 2020, **10**, 2142.
- 109 S. S. Das, P. Bharadwaj, M. Bilal, M. Barani, A. Rahdar, P. Taboada, S. Bungau and G. Z. Kyzas, *Polymers*, 2020, **12**, 1397.
- 110 T. C. Lim and M. Spector, *Transl. Stroke Res.*, 2017, **8**, 57–64.

- 111 X. Zhang, B. Gong, J. Zhai, Y. Zhao, Y. Lu, L. Zhang and J. Xue, *Chem. Res. Chin. Univ.*, 2021, **37**, 404–410.
- 112 W. Xue, C. Fan, B. Chen, Y. Zhao, Z. Xiao and J. Dai, *Stem Cells*, 2021, **39**, 1025–1032.
- 113 L. Huang and L. Zhang, *Prog. Neurobiol.*, 2019, **173**, 1–17.
- 114 C. Chen, J. Tang, Y. Gu, L. Liu, X. Liu, L. Deng, C. Martins, B. Sarmiento, W. Cui and L. Chen, *Adv. Funct. Mater.*, 2019, **29**, 1970024.
- 115 W. Tang, F. Fang, K. Liu, Z. Huang, H. Li, Y. Yin, J. Wang, G. Wang, L. Wei, Y. Ou and Y. Wang, *ACS Biomater. Sci. Eng.*, 2020, **6**, 2209–2218.
- 116 S. Yao, F. He, Z. Cao, Z. Sun, Y. Chen, H. Zhao, X. Yu, X. Wang, Y. Yang, F. Rosei and L. N. Wang, *ACS Biomater. Sci. Eng.*, 2020, **6**, 1165–1175.
- 117 A. Jakobsson, M. Ottosson, M. C. Zalis, D. O'Carroll, U. E. Johansson and F. Johansson, *Nanomedicine*, 2017, **13**, 1563–1573.
- 118 Y. Wang, H. Tan and X. Hui, *BioMed Res. Int.*, 2018, **2018**, 7848901.
- 119 S. Chen, J. V. John, A. McCarthy and J. Xie, *J. Mater. Chem. B*, 2020, **8**, 3733–3746.
- 120 W. Zhong, X. Zhang, Y. Zeng, D. Lin and J. Wu, *Nano Res.*, 2021, **14**, 2067–2089.
- 121 M. S. Karizmeh, S. A. Poursamar, A. Kefayat, Z. Farahbakhsh and M. Rafienia, *Mater. Sci. Eng., C*, 2022, DOI: [10.1016/j.msec.2022.112667](https://doi.org/10.1016/j.msec.2022.112667).
- 122 S. MacNeil, *Nature*, 2007, **445**, 874–880.
- 123 A. Keirouz, M. Chung, J. Kwon, G. Fortunato and N. Radacsi, *Wiley Interdiscip. Rev.: Nanomed. Nanobiotechnol.*, 2020, **12**, e1626.
- 124 F. Groeber, M. Holeiter, M. Hampel, S. Hinderer and K. Schenke-Layland, *Adv. Drug Delivery Rev.*, 2011, **63**, 352–366.
- 125 M. Sheikholeslam, M. E.-E. Wright, M. G. Jeschke and S. Amini-Nik, *Adv. Healthcare Mater.*, 2018, **7**, 1700897.
- 126 F. Ahmadi-Aghkand, S. Gholizadeh-Ghaleh Aziz, Y. Panahi, H. Daraee, F. Gorjikhah, S. Gholizadeh-Ghaleh Aziz, A. Hsanazadeh and A. Akbarzadeh, *Artif. Cells Nanomed. Biotechnol.*, 2016, **44**, 1635–1641.
- 127 R. Ekambaram and S. Dharmalingam, *Mater. Sci. Eng., C*, 2020, **115**, 111150.
- 128 A. Cipitria, A. Skelton, T. R. Dargaville, P. D. Dalton and D. W. Huttmacher, *J. Mater. Chem.*, 2011, **21**, 9419.
- 129 K. S. Ogueri and C. T. Laurencin, *ACS Nano*, 2020, **14**, 9347–9363.
- 130 Y. Su, M. S. Toftdal, A. Le Fricc, M. Dong, X. Han and M. Chen, *Small Sci.*, 2021, **1**, 2100003.
- 131 W. A. Sarhan, H. M. Azzazy and I. M. El-Sherbiny, *ACS Appl. Mater. Interfaces*, 2016, **8**, 6379–6390.
- 132 S. S. Hosseini Salekdeh, H. Daemi, M. Zare-Gachi, S. Rajabi, F. Bazgir, N. Aghdami, M. S. Nourbakhsh and H. Baharvand, *ACS Appl. Mater. Interfaces*, 2020, **12**, 3393–3406.
- 133 W. Li, A. Q. Nie, Q. Li, N. Xie and Y. Z. Ling, *Mater. Express*, 2019, **9**, 484–491.
- 134 G. Han and R. Ceilley, *Adv. Ther.*, 2017, **34**, 599–610.
- 135 X. Zhao, P. Li, B. Guo and P. X. Ma, *Acta Biomater.*, 2015, **26**, 236–248.
- 136 J. He, Y. Liang, M. Shi and B. Guo, *Chem. Eng. J.*, 2020, **385**, 123464.
- 137 X. Zhang, R. Lv, L. Chen, R. Sun, Y. Zhang, R. Sheng, T. Du, Y. Li and Y. Qi, *ACS Appl. Mater. Interfaces*, 2022, **14**, 12984–13000.
- 138 D. Mushahary, R. Sravanthi, Y. Li, M. J. Kumar, N. Harishankar, P. D. Hodgson, C. Wen and G. Pande, *Int. J. Nanomed.*, 2013, **8**, 2887–2902.
- 139 W. K. Jung, H. C. Koo, K. W. Kim, S. Shin, S. H. Kim and Y. H. Park, *Appl. Environ. Microbiol.*, 2008, **74**, 2171–2178.
- 140 Y. Zhou, Y. Kong, S. Kundu, J. D. Cirillo and H. Liang, *J. Nanobiotechnol.*, 2012, **10**, 19.
- 141 M. A.-M. Hussein, M. Grinholc, A. S.-A. Dena, I. M. El-Sherbiny and M. Megahed, *Carbohydr. Polym.*, 2021, **256**, 117498.
- 142 X. Yang, J. Yang, L. Wang, B. Ran, Y. Jia, L. Zhang, G. Yang, H. Shao and X. Jiang, *ACS Nano*, 2017, **11**, 5737–5745.
- 143 C. Zhu, R. Cao, Y. Zhang and R. Chen, *Front. Cell Dev. Biol.*, 2021, **9**, 660571.
- 144 N. S. Greaves, K. J. Ashcroft, M. Baguneid and A. Bayat, *J. Dermatol. Sci.*, 2013, **72**, 206–217.
- 145 J. Etulain, *Platelets*, 2018, **29**, 556–568.
- 146 Y. Guo, J. Huang, Y. Fang, H. Huang and J. Wu, *Chem. Eng. J.*, 2022, **437**, 134690.
- 147 Y. Dong, Y. Zheng, K. Zhang, Y. Yao, L. Wang, X. Li, J. Yu and B. Ding, *Adv. Fiber Mater.*, 2020, **2**, 212–227.
- 148 Z. Zhu, Y. Liu, Y. Xue, X. Cheng, W. Zhao, J. Wang, R. He, Q. Wan and X. Pei, *ACS Appl. Mater. Interfaces*, 2019, **11**, 36141–36153.
- 149 H. Zigdon-Giladi, A. Khutaba, R. Elimelech, E. E. Machtei and S. Srouji, *J. Biomed. Mater. Res., Part A*, 2017, **105**, 2712–2721.
- 150 M. Champeau, V. Pova, L. Militao, F. M. Cabrini, G. F. Picheth, F. Meneau, C. P. Jara, E. P. de Araujo and M. G. de Oliveira, *Acta Biomater.*, 2018, **74**, 312–325.
- 151 P. Zhang, Y. Li, Y. Tang, H. Shen, J. Li, Z. Yi, Q. Ke and H. Xu, *ACS Appl. Mater. Interfaces*, 2020, **12**, 18319–18331.
- 152 T. Mehrabi, A. S. Mesgar and Z. Mohammadi, *ACS Biomater. Sci. Eng.*, 2020, **6**, 5399–5430.
- 153 S. Park, J. Kim, M. K. Lee, C. Park, H. D. Jung, H. E. Kim and T. S. Jang, *Mater. Des.*, 2019, **181**, 108079.
- 154 S. Werner, T. Krieg and H. Smola, *J. Invest. Dermatol.*, 2007, **127**, 998–1008.
- 155 V. Grotheer, M. Goergens, P. C. Fuchs, S. Dunda, N. Pallua, J. Windolf and C. V. Suschek, *Biomaterials*, 2013, **34**, 7314–7327.
- 156 M. Risbud, A. Hardikar and R. Bhone, *J. Biosci.*, 2000, **25**, 25–31.
- 157 P. Pal, P. K. Srivas, P. Dadhich, B. Das, D. Maulik and S. Dhara, *ACS Biomater. Sci. Eng.*, 2017, **3**, 3563–3575.
- 158 J. Du, Y. Yao, M. Wang, R. Su, X. Li, J. Yu and B. Ding, *Adv. Funct. Mater.*, 2022, **32**, 2109833.
- 159 J. Sun, C. Mou, Q. Shi, B. Chen, X. Hou, W. Zhang, X. Li, Y. Zhuang, J. Shi, Y. Chen and J. Dai, *Biomaterials*, 2018, **162**, 22–33.

- 160 Y. Li, Y. Xiao and C. Liu, *Chem. Rev.*, 2017, **117**, 4376–4421.
- 161 M. A. Laflamme and C. E. Murry, *Nature*, 2011, **473**, 326–335.
- 162 M. F. Tenreiro, A. F. Louro, P. M. Alves and M. Serra, *npj Regener. Med.*, 2021, **6**, 30.
- 163 A. Chen, D. K. Lieu, L. Freschauf, V. Lew, H. Sharma, J. Wang, D. Nguyen, I. Karakikes, R. J. Hajjar, A. Gopinathan, E. Botvinick, C. C. Fowlkes, R. A. Li and M. Khine, *Adv. Mater.*, 2011, **23**, 5785–5791.
- 164 H. N. Kim, A. Jiao, N. S. Hwang, M. S. Kim, D. H. Kang, D. H. Kim and K. Y. Suh, *Adv. Drug Delivery Rev.*, 2013, **65**, 536–558.
- 165 M. Suhaeri, R. Subbiah, S. H. Kim, C. H. Kim, S. J. Oh, S. H. Kim and K. Park, *ACS Appl. Mater. Interfaces*, 2017, **9**, 224–235.
- 166 S. Pascual-Gil, E. Garbayo, P. Diaz-Herraez, F. Prosper and M. J. Blanco-Prieto, *J. Controlled Release*, 2015, **203**, 23–38.
- 167 S. P. Kwon, B. H. Hwang, E. H. Park, H. Y. Kim, J. R. Lee, M. Kang, S. Y. Song, M. Jung, H. S. Sohn, E. Kim, C. W. Kim, K. Y. Lee, G. C. Oh, E. Choo, S. Lim, Y. Chung, K. Chang and B. S. Kim, *Small*, 2021, **17**, e2101207.
- 168 T. Hao, J. Li, F. Yao, D. Dong, Y. Wang, B. Yang and C. Wang, *ACS Nano*, 2017, **11**, 5474–5488.
- 169 Y. Zhu, Y. Matsumura, M. Velayutham, L. M. Foley, T. K. Hitchens and W. R. Wagner, *Biomaterials*, 2018, **177**, 98–112.
- 170 Z. Li, D. Zhu, Q. Hui, J. Bi, B. Yu, Z. Huang, S. Hu, Z. Wang, T. Caranasos, J. Rossi, X. Li, K. Cheng and X. Wang, *Adv. Funct. Mater.*, 2021, **31**, 2004377.
- 171 S. Huang and N. G. Frangogiannis, *Br. J. Pharmacol.*, 2018, **175**, 1377–1400.
- 172 T. Zhao, W. Wu, L. Sui, Q. Huang, Y. Nan, J. Liu and K. Ai, *Bioact. Mater.*, 2022, **7**, 47–72.
- 173 J. Li, W. Fang, T. Hao, D. Dong, B. Yang, F. Yao and C. Wang, *Composites, Part B*, 2020, **199**, 108285.
- 174 J. Xie, Y. Yao, S. Wang, L. Fan, J. Ding, Y. Gao, S. Li, L. Shen, Y. Zhu and C. Gao, *Adv. Healthcare Mater.*, 2022, **11**, e2101855.
- 175 W. Zhang, X. Hu, Q. Shen and D. Xing, *Nat. Commun.*, 2019, **10**, 1704.
- 176 Y. Yao, J. Ding, Z. Wang, H. Zhang, J. Xie, Y. Wang, L. Hong, Z. Mao, J. Gao and C. Gao, *Biomaterials*, 2020, **232**, 119726.
- 177 Y. F. Qi, J. Zhang, L. Wang, V. Shenoy, E. Krause, S. P. Oh, C. J. Pepine, M. J. Katovich and M. K. Raizada, *J. Mol. Med.*, 2016, **94**, 37–49.
- 178 Z. Qiu, J. Zhao, F. Huang, L. Bao, Y. Chen, K. Yang, W. Cui and W. Jin, *npj Regener. Med.*, 2021, **6**, 44.
- 179 T. Takada, D. Sasaki, K. Matsuura, K. Miura, S. Sakamoto, H. Goto, T. Ohya, T. Iida, J. Homma, T. Shimizu and N. Hagiwara, *Biomaterials*, 2022, **281**, 121351.
- 180 H. Parsa, K. Ronaldson and G. Vunjak-Novakovic, *Adv. Drug Delivery Rev.*, 2016, **96**, 195–202.
- 181 G. A. Mensah, G. A. Roth and V. Fuster, *J. Am. Coll. Cardiol.*, 2019, **74**, 2529–2532.
- 182 G. Zhao, X. Zhang, T. J. Lu and F. Xu, *Adv. Funct. Mater.*, 2015, **25**, 5726–5738.
- 183 N. Adadi, M. Yadid, I. Gal, M. Asulin, R. Feiner, R. Edri and T. Dvir, *Adv. Mater. Technol.*, 2020, **5**, 1900820.
- 184 M. Wanjare, L. Hou, K. H. Nakayama, J. J. Kim, N. P. Mezak, O. J. Abilez, E. Tzatzalos, J. C. Wu and N. F. Huang, *Biomater. Sci.*, 2017, **5**, 1567–1578.
- 185 J. Han, Q. Wu, Y. Xia, M. B. Wagner and C. Xu, *Stem Cell Res.*, 2016, **16**, 740–750.
- 186 S. Eom, S. M. Park, D. G. Hwang, H. W. Kim, J. Jang and D. S. Kim, *Composites, Part B*, 2021, **226**, 109336.
- 187 Y. Wu, L. Wang, B. Guo and P. X. Ma, *ACS Nano*, 2017, **11**, 5646–5659.
- 188 X. Zhang, L. Li, J. Ouyang, L. Zhang, J. Xue, H. Zhang and W. Tao, *Nano Today*, 2021, **39**, 101196.
- 189 L. Wang, Y. Wu, T. Hu, B. Guo and P. X. Ma, *Acta Biomater.*, 2017, **59**, 68–81.
- 190 B. Tian, J. Liu, T. Dvir, L. Jin, J. H. Tsui, Q. Qing, Z. Suo, R. Langer, D. S. Kohane and C. M. Lieber, *Nat. Mater.*, 2012, **11**, 986–994.
- 191 R. Feiner, L. Engel, S. Fleischer, M. Malki, I. Gal, A. Shapira, Y. Shacham-Diamand and T. Dvir, *Nat. Mater.*, 2016, **15**, 679–685.
- 192 C. A. Grant and P. C.-J. A.-N. Twigg, *ACS Nano*, 2012, **7**, 456–464.
- 193 S. Sarkar, T. Schmitz-Rixen, G. Hamilton and A. M. Seifalian, *Med. Biol. Eng. Comput.*, 2007, **45**, 327–336.
- 194 L. E. Niklason and J. H. Lawson, *Science*, 2020, **370**, 6513.
- 195 M. B. Browning, D. Dempsey, V. Guiza, S. Becerra, J. Rivera, B. Russell, M. Hook, F. Clubb, M. Miller, T. Fossum, J. F. Dong, A. L. Bergeron, M. Hahn and E. Cosgriff-Hernandez, *Acta Biomater.*, 2012, **8**, 1010–1021.
- 196 H. Kurobe, M. W. Maxfield, S. Tara, K. A. Rocco, P. S. Bagi, T. Yi, B. Udelsman, Z. W. Zhuang, M. Cleary, Y. Iwakiri, C. K. Breuer and T. Shinoka, *PLoS One*, 2015, **10**, e0120328.
- 197 N. Thottappillil and P. D. Nair, *Mater. Sci. Eng., C*, 2020, **114**, 111030.
- 198 L. Weidenbacher, E. Muller, A. G. Guex, M. Zundel, P. Schweizer, V. Marina, C. Adlhart, L. Vejsadova, R. Pauer, E. Spiecker, K. Maniura-Weber, S. J. Ferguson, R. M. Rossi, M. Rottmar and G. Fortunato, *ACS Appl. Mater. Interfaces*, 2019, **11**, 5740–5751.
- 199 W. G. Chang and L. E. Niklason, *npj Regener. Med.*, 2017, **2**, 7.
- 200 K. Wang, Q. Zhang, L. Zhao, Y. Pan, T. Wang, D. Zhi, S. Ma, P. Zhang, T. Zhao, S. Zhang, W. Li, M. Zhu, Y. Zhu, J. Zhang, M. Qiao and D. Kong, *ACS Appl. Mater. Interfaces*, 2017, **9**, 11415–11427.
- 201 S. Liu, C. Dong, G. Lu, Q. Lu, Z. Li, D. L. Kaplan and H. Zhu, *Acta Biomater.*, 2013, **9**, 8991–9003.
- 202 M. Moffa, A. G. Sciancalepore, L. G. Passione and D. Pisignano, *Small*, 2014, **10**, 2439–2450.
- 203 X. Dong, X. Yuan, L. Wang, J. Liu, A. C. Midgley, Z. Wang, K. Wang, J. Liu, M. Zhu and D. Kong, *Biomaterials*, 2018, **181**, 1–14.

- 204 Z. Liu, Z. Zheng, K. Chen, Y. Li, X. Wang and G. Li, *Colloids Surf., B*, 2019, **180**, 118–126.
- 205 I. S. Robu, H. L. Walters, 3rd and H. W.-T. Matthew, *J. Biomed. Mater. Res., Part A*, 2017, **105**, 1725–1735.
- 206 Q. Zhang, S. He, X. Zhu, H. Luo, M. Gama, M. Peng, X. Deng and Y. Wan, *Mater. Sci. Eng., C*, 2021, **122**, 111861.
- 207 D. Wang, X. Wang, X. Li, L. Jiang, Z. Chang and Q. Li, *Mater. Sci. Eng., C*, 2020, **107**, 110212.
- 208 Z. Yang, Q. Tu, Y. Zhu, R. Luo, X. Li, Y. Xie, M. F. Maitz, J. Wang and N. Huang, *Adv. Healthcare Mater.*, 2012, **1**, 548–559.
- 209 T. Y. Kang, J. M. Hong, B. J. Kim, H. J. Cha and D. W. Cho, *Acta Biomater.*, 2013, **9**, 4716–4725.
- 210 S. Oliveira, T. Felizardo, S. Amorim, S. M. Mithieux, R. A. Pires, R. L. Reis, A. Martins, A. S. Weiss and N. M. Neves, *Biomacromolecules*, 2020, **21**, 3582–3595.
- 211 D. Hao, Y. Fan, W. Xiao, R. Liu, C. Pivetti, T. Walimbe, F. Guo, X. Zhang, D. L. Farmer, F. Wang, A. Panitch, K. S. Lam and A. Wang, *Acta Biomater.*, 2020, **108**, 178–193.
- 212 R. Khosravi, C. A. Best, R. A. Allen, C. E.-T. Stowell, E. Onwuka, J. J. Zhuang, Y. U. Lee, T. Yi, M. R. Bersi, T. Shinoka, J. D. Humphrey, Y. Wang and C. K. Breuer, *Ann. Biomed. Eng.*, 2016, **44**, 2402–2416.
- 213 T. Yao, M. B. Baker and L. Moroni, *Nanomaterials*, 2020, **10**, 887.
- 214 X. Jia, C. Zhao, P. Li, H. Zhang, Y. Huang, H. Li, J. Fan, W. Feng, X. Yuan and Y. Fan, *J. Biomater. Sci., Polym. Ed.*, 2011, **22**, 1811–1827.
- 215 Y. T. Hu, X. D. Pan, J. Zheng, W. G. Ma and L. Z. Sun, *Int. J. Surg.*, 2017, **44**, 244–249.
- 216 D. Jin, J. Hu, D. Xia, A. Liu, H. Kuang, J. Du, X. Mo and M. Yin, *Int. J. Nanomed.*, 2019, **14**, 4261–4276.
- 217 T. Wu, J. Zhang, Y. Wang, D. Li, B. Sun, H. El-Hamshary, M. Yin and X. Mo, *Mater. Sci. Eng., C*, 2018, **82**, 121–129.
- 218 T. Nakamura, T. Inatomi, C. Sotozono, N. Koizumi and S. Kinoshita, *Prog. Retin. Eye Res.*, 2016, **51**, 187–207.
- 219 G. A. Silva, N. F. Silva and T. M. Fortunato, *Curr. Stem Cell Res. Ther.*, 2011, **6**, 255–272.
- 220 A. Pandhare, P. Bhatt and Y. Pathak, *Advanced 3D-Printed Systems and Nanosystems for Drug Delivery and Tissue Engineering*, 2020, pp. 255–275, DOI: [10.1016/b978-0-12-818471-4.00009-1](https://doi.org/10.1016/b978-0-12-818471-4.00009-1).
- 221 M. Doostmohammadi, H. Forootanfar and S. Ramakrishna, *Mater. Sci. Eng., C*, 2020, **109**, 110521.
- 222 A. Lotery and D. Trump, *Hum. Genet.*, 2007, **122**, 219–236.
- 223 J. C. Booij, D. C. Baas, J. Beisekeeva, T. G. Gorgels and A. A. Bergen, *Prog. Retin. Eye Res.*, 2010, **29**, 1–18.
- 224 E. B. Lavik, H. Klassen, K. Warfvinge, R. Langer and M. J. Young, *Biomaterials*, 2005, **26**, 3187–3196.
- 225 H. A. Thomson, A. J. Treharne, P. Walker, M. C. Gossel and A. J. Lotery, *Br. J. Ophthalmol.*, 2011, **95**, 563–568.
- 226 L. C. Lu, M. J. Yaszemski and A. G. Mikos, *Biomaterials*, 2001, **22**, 3345–3355.
- 227 S. R. Hynes and E. B. Lavik, *Graefes. Arch. Clin. Exp. Ophthalmol.*, 2010, **248**, 763–778.
- 228 B. Diniz, P. Thomas, B. Thomas, R. Ribeiro, Y. Hu, R. Brant, A. Ahuja, D. Zhu, L. Liu, M. Koss, M. Maia, G. Chader, D. R. Hinton and M. S. Humayun, *Invest. Ophthalmol. Vis. Sci.*, 2013, **54**, 5087–5096.
- 229 N. Yaji, M. Yamato, J. Yang, T. Okano and S. Hori, *Biomaterials*, 2009, **30**, 797–803.
- 230 A. O. Eghrari, S. A. Riazuddin and J. D. Gottsch, *Prog. Mol. Biol. Transl. Sci.*, 2015, **134**, 7–23.
- 231 M. Yamato, *Drug Delivery Syst.*, 2006, **21**, 623–626.
- 232 M. R. Atallah, S. Palioura, V. L. Perez and G. Amescua, *Clin. Ophthalmol.*, 2016, **10**, 593–602.
- 233 P. Rama, S. Matuska, G. Paganoni, A. Spinelli, M. De Luca and G. Pellegrini, *N. Engl. J. Med.*, 2010, **363**, 147–155.
- 234 A. Baradaran-Rafii, E. Biazar and S. Heidari-Keshel, *ASAIO J.*, 2015, **61**, 605–612.
- 235 B. Kong, W. Sun, G. Chen, S. Tang, M. Li, Z. Shao and S. Mi, *Sci. Rep.*, 2017, **7**, 970.
- 236 S. Sharma, D. Gupta, S. Mohanty, M. Jassal, A. K. Agrawal and R. Tandon, *Invest. Ophthalmol. Vis. Sci.*, 2014, **55**, 899–907.